Design and synthesis of dithiocarbamate linked β-carboline derivatives: DNA topoisomerase II inhibition with DNA binding and apoptosis inducing ability

ARTICLE *in* BIOORGANIC & MEDICINAL CHEMISTRY · JULY 2015

Impact Factor: 2.79 · DOI: 10.1016/j.bmc.2015.07.037

Bioorganic & Medicinal Chemistry 23 (2015) 5511–5526

Contents lists available at ScienceDirect

Bioorganic & Medicinal Chemistry

journal homepage: www.elsevier.com/locate/bmc

Design and synthesis of dithiocarbamate linked β-carboline derivatives: DNA topoisomerase II inhibition with DNA binding and apoptosis inducing ability

Ahmed Kamal [a,b,*], Manda Sathish [a], V. Lakshma Nayak [a], Vunnam Srinivasulu [a], Botla Kavitha [b], Yellaiah Tangella [a], Dinesh Thummuri [b], Chandrakant Bagul [a,b], Nagula Shankaraiah [b], Narayana Nagesh [c,*]

[a] Medicinal Chemistry & Pharmacology, CSIR-Indian Institute of Chemical Technology, Hyderabad 500 007, India
[b] Department of Medicinal Chemistry, National Institute of Pharmaceutical Education and Research (NIPER), Hyderabad 500 037, India
[c] CSIR-Centre for Cellular and Molecular Biology, Hyderabad 500 007, India

ARTICLE INFO

Article history:
Received 6 April 2015
Revised 17 July 2015
Accepted 19 July 2015
Available online 27 July 2015

Keywords:
β-Carboline
Dithiocarbamate
Topoisomerase II
Anticancer activity
DNA-binding affinity
Pharmacophore

ABSTRACT

A series of new β-carboline-dithiocarbamate derivatives bearing phenyl, dithiocarbamate and H/methyl substitutions at position-1, 3 and 9, respectively, were designed and synthesized. These derivatives **8a–l** and **13a–l** and their starting precursors (**7a–d** and **12a–d**) have been evaluated for their in vitro cytotoxic activity on selected human cancer cell lines. Among the derivatives tested, **7c**, **12c**, **8a**, **8d**, **8i**, **8j**, **8k**, **8l** and **13d–l** exhibited considerable cytotoxicity against most of the tested cancer cell lines (IC_{50} <10 μM). Interestingly, most of the derivatives (**8a–l** and **13a–l**) exhibited enhanced activity than their precursors (**7a–d** and **12a–d**), which indicates that the combination of dithiocarbamate with β-carboline enhances the cytotoxicity of **8a–l** and **13a–l**. Moreover, the derivatives **8j** and **13g** exhibited significant cytotoxic activity with IC_{50} values of 1.34 μM and 0.79 μM on DU-145 cancer cells, respectively. Further, the induction of apoptosis by these derivatives was confirmed by Annexin V-FITC and Hoechst staining assays. However, both biophysical as well as molecular docking studies suggested a combilexin-type of interaction between these derivatives and DNA, unlike simple β-carbolines. With a view to understand their mechanism of action, DNA topoisomerase II (topo II) inhibition assay was also performed. Overall, the present study emphasizes the importance of linking a dithiocarbamate moiety to the β-carboline scaffold for exhibiting profound activity.

1. Introduction

DNA is one of the most essential pharmacological targets of many drugs presently in clinical usage. Small molecules that bind to DNA have proven to be effective antiviral, antibacterial and anticancer therapeutic agents.[1] Many, small molecules could interact with DNA through (i) intercalation; (ii) surface binding; (iii) minor groove, and (iv) major groove binding.[2] An important class of drugs in anticancer therapy is DNA intercalators and the study of the interaction of such agents with DNA, in particular their structural basis could offer newer insights into the design of new DNA targeting anticancer drugs.[3] In addition, the combilexin class of molecules, with mixed DNA intercalation and DNA groove-binding properties are capable of enhancing DNA-binding affinity due to their double mode of DNA interaction, for example NetAmsa (**F**, Fig. 1).[4]

Presently, a large number of anticancer drugs that are in clinical use are derived from natural products, it is the rationale to design improved DNA-binding agents based on natural products (Fig. 1).[5] The β-carboline alkaloids are a large group of natural and synthetic indole alkaloids with a broad spectrum of biological and pharmaceutical profiles.[6] Recent reports have revealed that β-carbolines are potential anticancer agents, which exert their anticancer effects through different mechanisms such as DNA intercalation,[7,8] inhibition of DNA topoisomerase I and II,[9] CDK,[10] MK-2,[11] PLK1,[12] kinesin Eg5[13] and IKK.[14] Among these, DNA intercalation is one of the important mode of action in clinical oncology and some of such drugs are currently used for the treatment of various cancers.[15] β-Carbolines have been characterized as DNA intercalators due to the presence of planar polycyclic aromatic pharmacophore, which is capable of stacking between DNA base pairs.[16] Moreover, some of the β-carbolines act as DNA topoisomerase II (topo II) inhibitors, which damage the DNA.[9] Earlier reports have shown that β-carboline derivatives containing a phenyl group at position-1, some biologically active heterocyclic scaffolds, such as

* Corresponding authors. Tel.: +91 40 27193157; fax: +91 40 27193189.
E-mail address: ahmedkamal@iict.res.in (A. Kamal).

http://dx.doi.org/10.1016/j.bmc.2015.07.037
0968-0896/

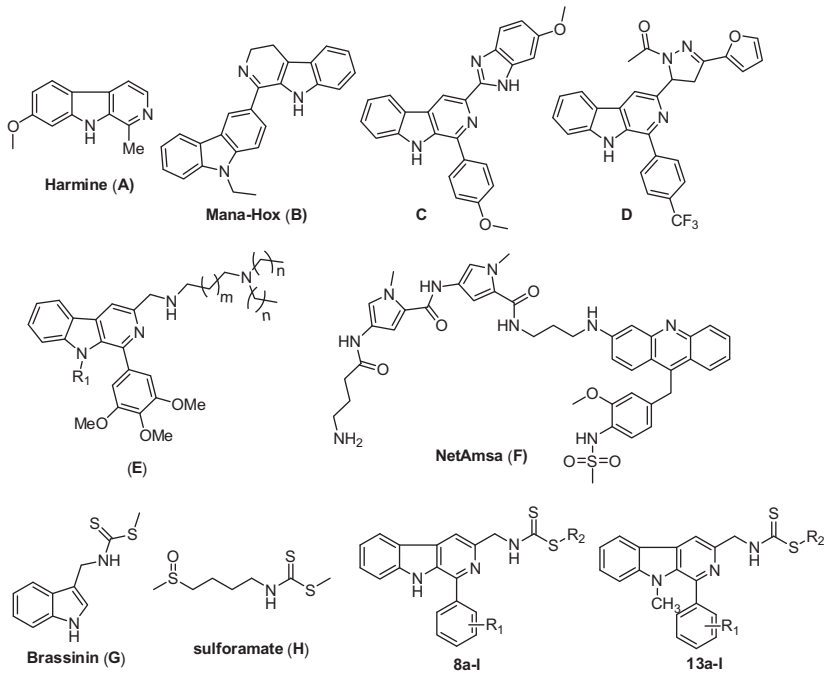

Figure 1. Pharmaceutically important β-carboline derivatives (A–E), combilexin molecule (F), dithiocarbamate derivatives (G and H) and synthesized derivatives (**8a–l** and **13a–l**).

1,3,4-oxadiazole,[17] 1,2,4-triazole,[17] 4-benzylidene-4*H*-oxazol-5-one,[18] or a substituted carbohydrazide[19] moiety at position-3 and some alkyl or aryl substitutions at position-9 demonstrated significant anticancer properties.[20] In addition, Chen and co-workers have reported that 3-chlorobenzyl and 3-phenylpropyl substituents at position-9 of β-carbolines showed significant anticancer activity.[20] Ikeda and co-workers have also reported 3-benzylamino-β-carboline derivatives as potential anticancer agents[21] and their SAR analysis revealed that (i) the common β-carboline skeleton is very important for the cytotoxic activity; (ii) the introduction of appropriate substitution at positions-1, 3 and 9 of the β-carboline nucleus enhanced the cytotoxic activity.[22] Recently, we have reported various β-carboline derivatives bearing different substituents at positions-1 and 3 of the β-carboline nucleus as promising cytotoxic agents.[23,24]

On the other hand, dithiocarbamates are a common class of organic molecules that display a wide range of biological activities such as antibacterial, antifungal and anticancer activities.[25] Moreover, brassinin (**G**, Fig. 1),[26,27] an indole based dithiocarbamate isolated from cruciferous vegetables such as Chinese cabbage, was found to be a significant chemopreventive agent.[27] Similarly, sulforamate (**H**, Fig 1) is another potent phase II enzyme inducer that could be used as a cancer chemopreventive agent.[28] However, the structure activity relationship (SAR) of brassinin revealed that chemopreventive nature was due to the dithiocarbamate motif and not the indole ring.[27]

In continuation of our earlier attempts toward the discovery of new molecules, we have developed a number of conjugate/derivative based scaffolds as potent anticancer agents.[29] In this context, a series of new β-carboline-3-methyl amines (**7a–d** and **12a–d**) and β-carboline-dithiocarbamate derivatives (**8a–l** and **13a–l**) respectively have been designed, synthesized and evaluated for their cytotoxic potential as well as DNA-binding ability. Furthermore, the in silico study of the absorption, distribution, metabolism and excretion (ADME) properties of these derivatives (**8a–l** and **13a–l**) were carried out by investigating Lipinski's parameters, topological polar surface area (TPSA) and percentage of absorption (% ABS).

2. Results and discussion

2.1. Chemistry

These β-carboline-dithiocarbamate derivatives **8a–l** and **13a–l** were synthesized as shown in Scheme 1. The L-tryptophan methyl ester (**2**) was obtained by esterification of L-tryptophan (**1**) by using $SOCl_2$. Pictet–Spengler condensation of **2** with various substituted benzaldehydes by employing *p*-TSA on refluxing yielded the corresponding methyl tetrahydro-β-carboline-3-carboxylates (**3a–d**) which were directly used for further aromatization with trichloroisocyanuric acid (TCC) to afford the fully aromatized methyl-β-carboline-3-carboxylates (**4a–d**). The N-methylation of **4a–d** by methyl iodide and sodium hydride afforded the 9-methyl-β-carboline-3-carboxylates (**9a–d**) in good yields. Next, the reduction of **4a–d** and **9a–d** with $LiBH_4$ in dry THF afforded the corresponding alcohols **5a–d** and **10a–d**, respectively, which were taken up for further azidation with diphenylphosphoryl azide and DBU to provide the corresponding azides **6a–d** and **11a–d** respectively. Then, Staudinger reduction of azide **6a–d** and **11a–d** to the corresponding amines was achieved by triphenylphosphene in acetonitrile and water to afford both 9-H and 9-methyl-β-carboline-3-methyl amine (**7a–d** and **12a–d**). Finally, the desired dithiocarbamate linked β-carboline derivatives (**8a–l** and **13a–l**) were obtained in good yields by the reaction of **7a–d** and **12a–d** with carbon disulfide, alkyl halides (methyl iodide, allyl bromide and benzyl bromide) and TEA in pyridine.

2.2. Biology

2.2.1. Cytotoxic activity

To evaluate the cytotoxicity of β-carboline-3-methyl amines (**7a–d** and **12a–d**) and the dithiocarbate linked β-carboline

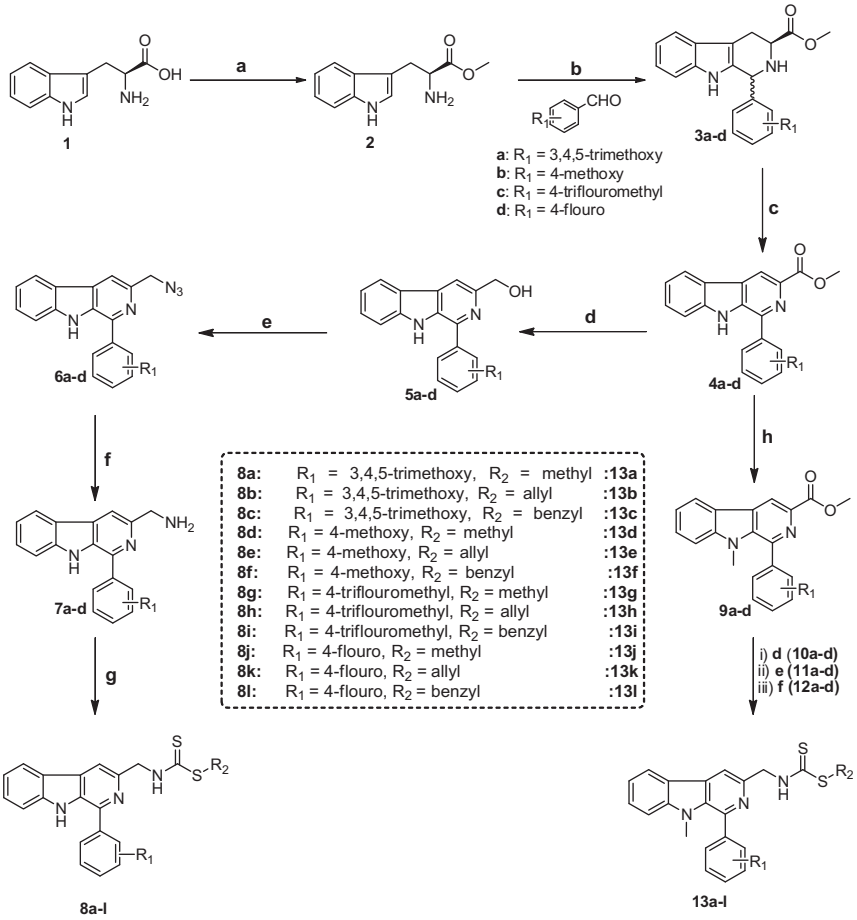

Scheme 1. Reagents and conditions: (a) $SOCl_2$, MeOH, 0 °C–rt, 12 h, 90%; (b) substituted benzaldehyde, *p*-TSA, EtOH, reflux, 12 h; (c) TCC, TEA, DMF, 0 °C–rt, 2 h, 70–85%; (d) $LiBH_4$, THF, 0 °C–rt, 4 h; (e) DPPA, DBU, dry THF, rt, 16 h, 60–80%; (f) TPP, acetonitrile/water (1:1), rt, 12 h, 55–70%; (g) alkyl halide, CS_2, TEA, pyridine, 0 °C, 30 min, 80–95%; (h) MeI, NaH, dry DMF, 0 °C, 4 h, 70–90%.

derivatives (**8a–l** and **13a–l**) MTT assay[30] was carried out on the selected human cancer cell lines, such as lung cancer (A549), breast cancer (MCF-7), prostate cancer (DU-145), and cervical cancer (HeLa). The cytotoxicity results are expressed in IC_{50} values that are tabulated in Table 1 and compared with the positive control doxorubicin. It is evident that most of the derivatives exhibited moderate to good cytotoxicity against the cancer cell lines tested, with IC_{50} values ranging from <1.0 μM to 60 μM. Among the derivatives, **8a**, **8d**, **8i–l** and **13d–l** exhibited considerable cytotoxicity against all the cancer cell lines (<10.0 μM). The most active derivatives in this series are **8d**, **8j**, **13d**, **13j**, **13g** and **13h** with IC_{50} values ranging from <1 μM to 2.0 μM. However, most of these derivatives showed higher cytotoxicity on DU-145 (prostate cancer) cell line in comparison to other cell lines. Derivatives **8j** and **13g** were found to be the most effective derivatives among the series exhibiting IC_{50} value of 1.34 and 0.79 μM, respectively, against DU-145 cell line and have also shown considerable activity against the other cell lines tested.

Based on the cytotoxicity assay, it is observed that the activity depends upon the substitution at positions 1, 3 and 9 of the β-carboline as well as on the nature of the substituents present on the phenyl ring (R_1) at position-1, substituents on the dithiocarbamate (R_2) and also H/Me at position-9 of β-carboline. Overall, the cytotoxicity of β-carboline-3-methyl amines (**7a–d** and **12a–d**) was comparatively lower than the dithiocarbamate linked β-carboline derivatives (**8a–l** and **13a–l**), indicating that the enhanced cytotoxicity of **8a–l** and **13a–l** is due to the attachment of dithiocarbamate side chain. Moreover, the new derivatives with a fluoro and trifluoromethyl (**8g–l** and **13g–l**) substituent on the phenyl ring at position-1 have shown significant cytotoxicity, probably due to the lipophilic nature of fluorine. Methyl dithiocarbamate linkage at position-3 of the β-carboline (incase of **8a**, **8d**, **8g**, **8j**, **13a**, **13d**, **13g** and **13j**) enhanced the cytotoxic activity in comparison to the other derivatives, thus indicates the importance of dithiocarbamate group. Furthermore, methyl substitution on position-9 also plays a crucial role for activity as all the 9-methyl β-carboline derivatives (**13a–l**) synthesized are most active with IC_{50} values <20 μM than the 9-H β-carboline derivatives (**8a–l**) with IC_{50} values <60 μM. Other derivatives possessing 3,4,5-trimethoxy and 4-methoxy at R_1, as well as allyl and benzyl at R_2 (**8a**, **8d**, **13a** and **8d** and **8f**) were also considerably active against most of the cell lines tested. However, derivative with a 4-methoxy substituent at R_1 and allyl substituent at R_2 (**8e**) was less active with IC_{50} value of >30 μM in this series. These results imply that the methyl group at R_2 represents the most appropriate structure for this class of derivatives, which displays remarkable cytotoxic activity. From the SAR studies, some interesting observations were made, such as trifluoromethyl and fluoro substitutions on the phenyl ring (R_1) at position-1 and a methyldithiocarbamate group at position-3 of the β-carboline is crucial for cytotoxicity, nevertheless some derivatives with methyl group at position-9 also display potent cytotoxicity.

2.2.2. Cell cycle analysis

To understand the effect of the active derivatives on cell cycle progression, cell cycle analysis was performed on DU-145 cell line. On treatment of DU-145 cells with 0.5 μM concentrations of **8j** and

Table 1
Cytotoxicity (IC_{50} values in μM)[a] of β-carboline-3-methylamines (**7a–d** and **12a–d**) and β-carboline-dithiocarbamate derivatives **8a–l** and **13a–l** on selected human cancer cell lines

Compound	A549[b]	MCF-7[c]	DU-145[d]	Hela[e]
7a	15.13	18.62	18.26	21.66
7b	17.84	18.91	17.39	18.59
7c	15.84	12.02	9.12	15.76
7d	21.10	17.95	13.77	22.50
12a	18.15	15.13	14.77	19.95
12b	20.09	16.62	12.78	14.79
12c	19.19	11.74	7.76	15.07
12d	19.49	16.59	10.00	20.51
8a	8.12	8.91	5.62	11.3
8b	12.8	15.8	13.8	23.2
8c	27.5	25.8	17.3	14.5
8d	7.94	8.51	1.14	7.78
8e	51.4	38.8	46.7	59.1
8f	17.7	10.0	13.8	24.1
8g	16.9	15.8	9.54	12.6
8h	18.6	10.9	7.76	10.6
8i	9.33	12.3	5.88	3.98
8j	4.36	2.45	1.34	3.46
8k	16.7	6.60	3.98	4.46
8l	39.8	7.41	3.71	3.81
13a	12.5	15.2	6.16	16.9
13b	18.1	20.6	19.4	19.9
13c	14.1	13.9	10.6	12.3
13d	5.12	1.51	1.41	2.57
13e	10.0	3.20	2.50	8.30
13f	9.12	3.36	6.91	13.8
13g	3.54	1.09	0.79	1.47
13h	4.26	4.78	1.99	4.67
13i	5.12	4.31	2.08	4.78
13j	5.62	1.86	1.45	2.39
13k	6.02	3.01	2.88	2.57
13l	6.76	2.75	4.78	3.16
Doxorubicin[f]	1.58	0.96	1.38	2.63

[a] 50% inhibitory concentration after 48 h of drug treatment and the values are average of three individual experiments.
[b] Human lung cancer (A549).
[c] Human breast cancer (MCF-7).
[d] Human prostate cancer (DU-145).
[e] Human cervical cancer (HeLa) cells.
[f] Doxorubicin was included as reference agent.

13g, a small increment in population of cells at sub-G1 stage (7.3% and 10.2%) was observed compared to control cells (6.5%). Whereas, on doubling the **8j** and **13g** concentrations (1.0 μM), the population of cells in sub-G1 further increased to 15.6% and 18.6%, respectively. These results imply that the cell cycle arrests at the sub-G1 phase and thereby induces cellular apoptosis.[31] The cell cycle histograms obtained for treatment of **13g** and **8j** at 0.5 μM and 1 μM concentrations are shown in Figure 2 and the results are displayed in Table 2.

2.2.3. Apoptosis induction studies

2.2.3.1. Annexin V-FITC. To further confirm the effect of **8j** and **13g** in inducing apoptosis, Annexin V-FITC/PI (AV/PI) dual staining assay was performed. This study is also useful to examine the occurrence of phosphatidylserine externalization as well as to find out whether it is due to physiological apoptosis or nonspecific necrosis.[32] Phosphatidylserine is used as a marker for cell death, moving from the inner cell membrane to the outer cell membrane during the cascade of apoptosis.[33] Annexin V is a cellular protein of the annexin group which selectively binds to phosphatidylserine.

In this study, DU-145 cells were treated with **8j** and **13g** for 48 h at 0.5 and 1.0 μM concentrations, and we found that these derivatives demonstrated significant apoptosis, as tabulated in Table 3 and dot plots are shown in Figure 3. The results indicated that **8j** and **13g** showed 19.0% and 23.3% apoptosis at a concentration of 1.0 μM, whereas 1.9% of apoptosis was observed in the control, this shows that derivative **13g** is a better inducer of apoptosis than **8j**.

2.2.3.2. Hoechst staining. Apoptosis is one of the main pathways that lead to cell death in which the chromatin condensation and fragmented nuclei are known as the classic characteristics.[34] Flow cytometry experiments demonstrated that **8j** and **13g** were effective in inducing apoptosis on DU-145 cells. Further, to visualize the apoptosis-inducing effect of such derivatives, Hoechst (H33258) staining was performed in DU-145 cells. Manual field quantification of apoptotic cells based on the presence of apoptotic bodies, cellular condensation, and nuclear fragmentation under the microscope in the presence of tested derivatives **8j** and **13g** showed a significant increase in the percentage of apoptotic cells in treated cells compared to the control. However, this study shows that **13g** is more effective than **8j** in causing apoptosis as more number of wrinkled and DNA fragmented cells were observed in cells treated with **13g** (0.5 μM) than in **8j** (0.5 μM) as shown in Figure 3.

2.2.4. DNA-topoisomerase II inhibition study

DNA-topoisomerase II (topo II) is a nuclear enzyme that controls the DNA structure by catalyzing the DNA cleavage and relegating the phosphodiester bonds. In recent years, DNA topo II inhibitors have gained importance as clinically useful chemotherapeutic agents. Topo II inhibition studies were performed by using topo II Drug Screening Kit (TG 1009, Topogen, USA), which is suitable for screening the enzyme inhibition by both catalytic inhibitory compounds (CICs) and interfacial poisons (IFPs). CICs inhibit the activity of the enzyme, whereas IFP compounds stimulate the formation of the cleavage complexes and block the relegation which leads to form linear DNA. Catenated DNA in the presence of topo II enzyme incubated with etoposide at concentration of 1, 10 and 100 μM (lane E to G in control, Fig. 4) showed clear linear DNA formation indicating that it acts as IFP which blocks the resealing of the dsDNA. Catenated DNA in the presence of topo II enzyme incubated with compound **8j** (lane E to G in **8j**, Fig. 4) at concentration of 1–100 μM did not show the formation of linear DNA, but most of the catenated DNA was highly super coiled and remained in the wells documenting the formation of only nicked circular and relaxed DNA, indicated that the compounds interference in the catalytic activity of the topo II enzyme and suggesting that the role of **8j** as CIC. Further, catenated DNA in the presence of topo II incubated with compound **13g** showed the formation of linear DNA at concentrations of 1–100 μM in a similar pattern to etoposide indicating that it acts as IFP (lane E to G in **13g**, Fig. 4). This assay indicates that both derivatives **8j** and **13g** affect the topo II enzyme activity, however derivative **8j** acts as CIC while derivative **13g** acts as IFP.

2.2.5. DNA binding studies

To further substantiate the biological activities of these active derivatives (**8j** and **13g**) and to understand the nature of interaction with DNA, spectroscopic studies were performed.

2.2.5.1. UV–visible spectroscopy. In order to investigate the nature of binding of these derivative molecules to DNA, the UV absorption spectra of active derivatives **8j** and **13g** in the presence and absence of increasing concentrations of CT DNA were examined (Fig. 5). On addition of DNA to derivative solution (**8j** or **13g**) the absorption band at 210 nm intensity gradually increases without exhibiting any shift, whereas the absorption band at 340 nm showed gradual decrease for derivative **8j** and slight decrease for derivative **13g** in its intensity. Since the absorption band at 210 nm shows hyperchromicity upon addition of DNA, it is evident that these derivatives could bind to the surface of

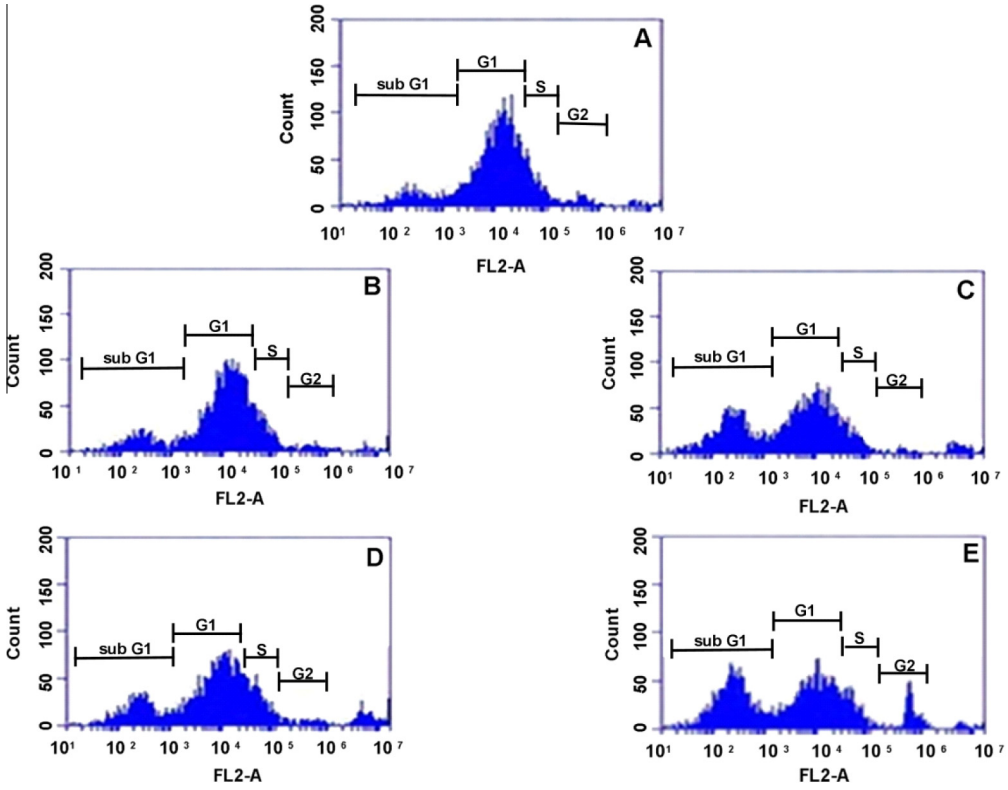

Figure 2. Flow cytometric analysis in DU-145 prostate cancer cell lines after treatment with derivatives **8j** and **13g** and 0.5 and 1 μM concentrations for 48 h; (A) control cells (DU-145); (B) **8j** (0.5 μM); (C) **8j** (1.0 μM); (D) **13g** (0.5 μM) and (E) **13g** (1.0 μM).

Table 2
Cell cycle results obtained when DU-145 cells were treated with 0.5 μM and 1.0 μM concentration of **8j** and **13g**

Sample	Sub G1 (%)	G0/G1 (%)	S (%)	G2/M (%)
A: Control	6.52	85.94	4.02	1.97
B: **8j** (0.5 μM)	7.34	84.83	3.36	1.98
C: **8j** (1 μM)	15.61	75.52	3.34	2.33
D: **13g** (0.5 μM)	10.12	78.90	5.18	3.73
E: **13g** (1 μM)	18.60	70.81	5.31	5.36

DNA,[35] however hypochromicity of absorption band at 340 nm indicates partial intercalation to DNA.[36] Interestingly, this data indicates that **8j** and **13g** exhibit combilexin-type of interaction with the DNA. However, the extent of variation in absorption band intensity at 210 nm and 340 nm is more with **8j** than **13g**, emphasizing higher ability of **8j** to interact with the DNA.

2.2.5.2. Fluorescence spectroscopy. Fluorescence titration is another valuable technique to understand the binding mode of small molecules to DNA at comparatively lower concentrations.[37] As these derivative molecules show fluorescence properties, their interaction with CT-DNA could provide certain observations regarding the nature of their interactions with DNA. In this study, when CT-DNA was added to the derivative, the fluorescence emission peak of **8j** and **13g**, exhibited hypochromicity. Hypochromicity of the fluorescence emission peak was observed at 617 and 567 nm for the **8j** and **13g**, respectively, indicating that the fluorescence of each derivative molecule getting quenched due to its interaction with CT-DNA. The quenching may be due to energy transfer from excited derivative molecules to the DNA bases. Fluorescence titration results indicate that these derivative molecules may intercalate between the DNA bases.[38] The fluorescence spectra recorded on the interaction of **8j** and **13g** with CT-DNA was depicted in Figure 5. Among **8j** and **13g**, the extent of quenching of emission band intensities is more with **8j**, indicating its higher level of intercalation with CT-DNA. Most of the catalytic inhibitory compounds (CICs) are strong intercalators and probably **8j** acts as a CIC due to its higher intercalation with DNA (as demonstrated by fluorescence studies).

Table 3
Percentage of apoptotic cells observed when DU-145 cells were treated with 0.5 and 1.0 μM concentrations of **8j** and **13g**

Sample	UL (%)	UR (%)	LL (%)	LR (%)
A: Control	0.10	1.52	97.95	0.43
B: **8j** (0.5 μM)	0.14	4.17	94.63	1.07
C: **8j** (1 μM)	0.96	14.68	79.95	4.40
D: **13g** (0.5 μM)	0.93	13.70	81.55	3.82
E: **13g** (1 μM)	1.65	21.19	74.99	2.18

2.2.5.3. Circular dichroism spectroscopy. The circular dichroism (CD) is a potential technique to study the nucleic acid conformational change due to interaction of DNA with molecules or changes in environmental conditions.[39] The CD spectrum of the calf thymus DNA (CT DNA) exhibits a positive band at 275 nm and a negative band at 245 nm due to π–π base stacking and right-hand helicity. On the addition of **8j** at a concentration of 10 μM to the same concentration of CT DNA solution (DNA/**8j** ligand, 1:1), positive band at 275 nm exhibits slight hyperchromicity, which is an indication of stabilization of the DNA–ligand complex.[40,41] Interestingly, on further increasing the concentration of **8j** (DNA/**8j** ligand, 1:2) the positive band at 275 nm also increases its intensity, indicating further stabilization of the DNA on ligand binding. Interestingly, a similar interaction was observed when **13g** was added to the CT-DNA solution, the positive CD band at 275 nm exhibited continuous hyperchromicity at both lower and higher concentrations, demonstrating complex stabilization. The

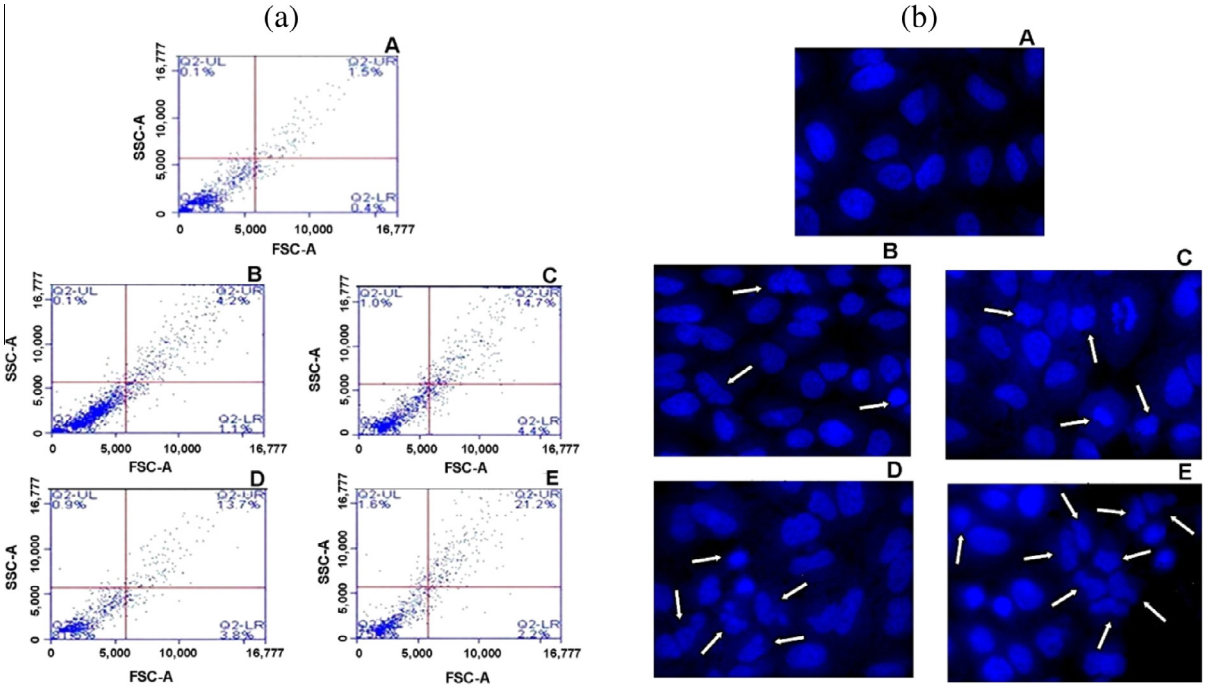

Figure 3. (a) Annexin V-FITC/PI (AV/PI) dual staining assay. (b) Hoechst (H33258) staining assay.

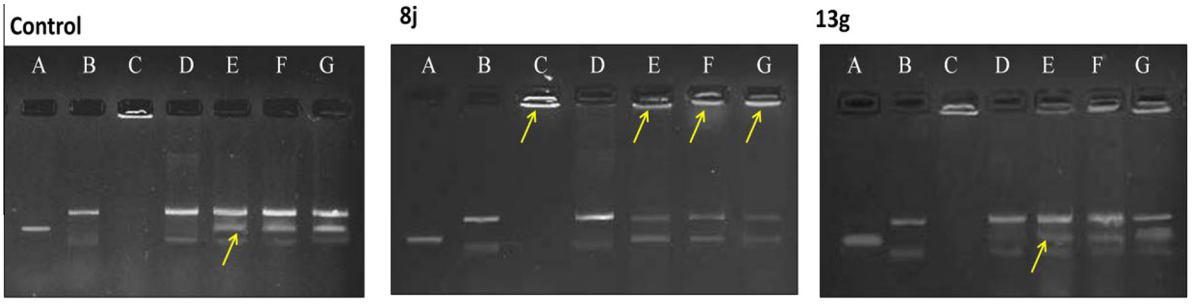

Figure 4. Effect of **8j** and **13g** on topo II inhibition.

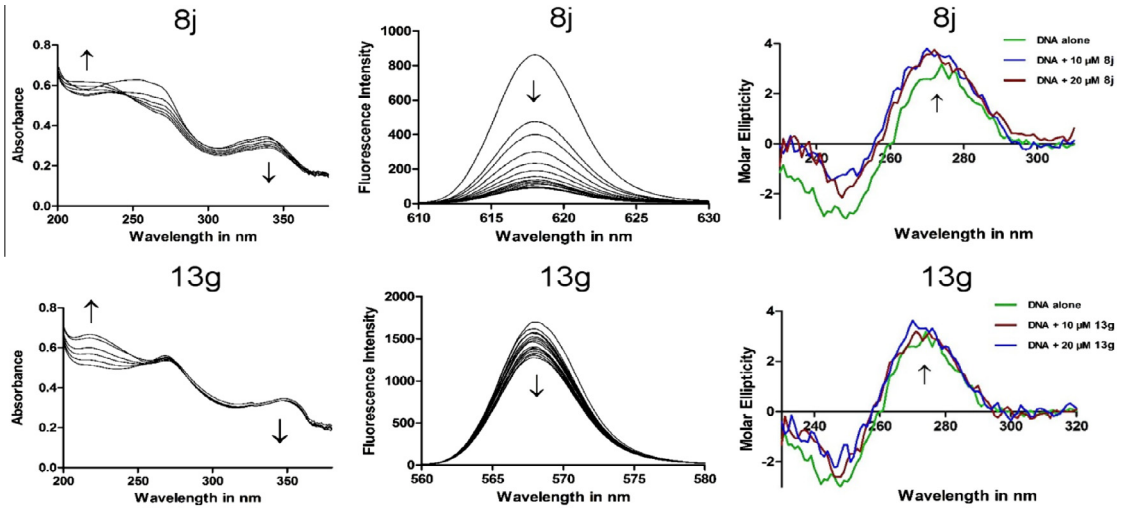

Figure 5. UV–visible spectra (left), fluorescence spectra (middle) and CD spectra (right) of derivatives **8j** and **13g**.

negative band intensity at 245 nm reduced to a greater extent with **8j** compared to **13g**, indicating its highest ability to minimize DNA staking. From Figure 5, it is evident that hyperchromicity is more in case of **8j**, indicating its higher potential to stabilize CT-DNA by intercalation, compared to **13g**, which may be due to its planarity.

2.3. In silico computational studies

An in silico computational study of the representative substituted dithiocarbamate linked β-carboline derivatives **8a–l** and **13a–l** was performed for determining the Lipinski's parameters, topological polar surface area (TPSA) and percentage of absorption (% ABS).[42] Calculations were performed by using the Molinspiration Online Property Calculation Toolkit (http://www.molinspiration.com).[43] The percentage of absorption was estimated by using the equation: % ABS = 109 − 0.345 × TPSA and the data generated are shown in Table 4. In vivo absorption of the newly synthesized β-carboline-dithiocarbamate derivatives was tentatively assessed by means of theoretical calculations following Lipinski's rule of five, which implies that the absorption or permeation of an orally administered compound is more likely to be better if the molecule satisfies the following rules: (i) hydrogen bond donors ⩽5 (OH and NH groups); (ii) hydrogen bond acceptors ⩽10 (N and O atoms); (iii) molecular weight <500; (iv) calculated log*P* <5.[42] Compounds that violate more than one of these rules could have problems related to bioavailability.

Most of these new derivatives violated only one of the Lipinski's rules, except **8c**, **8i**, **13c** and **13i**. Gratifyingly, the derivatives such as **8a**, **8j**, and **13a** in this series satisfied all the Lipinski's rules. Furthermore, derivatives that violated Lipinski's rules either have an octanol–water partition coefficients (log*P*) >5.0 or molecular weight larger than 500 Da only. All these derivatives have a number of hydrogen bond acceptors between 3 and 6 and 1–2 hydrogen bond donors respectively and these values are in agreement with the Lipinski's rules. Moreover, the calculated percentage of absorption of all derivatives ranged between 29.8% and 68.4%, demonstrating that these new derivatives may have the required cell membrane permeability.

Table 4
Lipinski's parameters for derivatives **8a–l** and **13a–l**

Compound	TPSA	Lipinsk's parameters				
		nHBA (NO)	nHBD (OHNH)	log*P*	MW	No. violations
8a	68.412	6	2	4.623	453.589	0
8b	68.412	6	2	5.267	479.627	1
8c	68.412	6	2	6.218	529.687	2
8d	49.944	4	2	5.048	393.537	1
8e	49.944	4	2	5.693	419.575	1
8f	49.944	4	2	6.643	469.635	1
8g	40.71	3	2	5.887	431.508	1
8h	40.71	3	2	6.532	457.546	1
8i	40.71	3	2	7.482	507.606	2
8j	40.71	3	2	5.155	381.501	0
8k	40.71	3	2	5.80	407.537	1
8l	40.71	3	2	6.750	457.599	1
13a	57.555	6	1	4.691	467.616	0
13b	57.555	6	1	5.335	493.654	1
13c	57.555	6	1	6.285	543.714	2
13d	39.087	4	1	5.116	407.564	1
13e	39.087	4	1	5.761	433.602	1
13f	39.087	4	1	6.711	483.662	1
13g	29.853	3	1	5.955	445.535	1
13h	29.853	3	1	6.599	471.573	1
13i	29.853	3	1	7.55	521.633	2
13j	29.853	3	1	5.223	395.528	1
13k	29.853	3	1	5.868	421.566	1
13l	29.853	3	1	6.818	471.626	1

2.4. Molecular docking studies

Most of the β-carboline derivatives that bind to topoisomerase enzyme, results in significant anticancer activity.[9] In the present study, the derivatives **8j** and **13g** have shown better topo II inhibition and cytotoxicity on selected human cancer cell lines. These results are encouraged us to perform molecular docking studies to understand the binding mode of these new derivatives to the different targets. Herein, all the co-ordinates of the crystal structures were obtained from Protein Data Bank. Necessary corrections to the protein and DNA structures were carried out by using Protein Preparation Wizard from Schrödinger package. Geometry optimization of these derivatives was carried out by Gaussian 09 package using PM3 semiempirical method.[44] All the docking studies were performed using AutoDock 4.2 docking software[45] and results were visualized through PyMOL.[46] These studies were performed on the new derivatives (**8a–l** and **13a–l**) and their amine intermediates (**7a–d** and **12a–d**) at the ATP binding site of the Topo-II (PDB ID 1ZXN).[47] Docking studies showed that these molecules fit well in the ATP binding site of the Topo-II (Fig. 6). Superimposed pose of the **13g** and co-crystallize ligand shown phosphate groups of the ADP and methyldithiocarbamate group was at the same position and β-carboline ring and nucleoside group of co-crystallized ligand was at the same position. However, β-carboline ring forms a T-type π–π stacking interaction with Phe142. Besides this, methyldithiocarbamate forms a hydrophobic contact with the Ile141, Thr147, Ser148, Gly161, Arg162, Asn163, Gly164, Tyr165, Gly166, and Ala167 amino acids and two hydrogen-bonding interactions with Gly166 and Ser148. Further, β-carboline ring forms a hydrophobic interaction with Tyr34, Ile88, Asn91, Ala92, Asn95, Ilu118, Asn120, Ile125, Tyr215 and Ile217 amino acids.

However, trifluoromethylphenyl ring forms a hydrophobic interaction with Asp94, Arg98, Ser149, Asn150, Lys157 and Thr159. In view of the biological activity, it is observed that the derivatives with 9-methyl substitution (**13a–l**) having the higher activity than the 9-H substitution (**8a–l**). To understand the binding poses of these derivatives, the both series (**8a–l** and **13a–l**) were examined. Superimposed poses of **8g** and **13g** (with 9-methyl substituent) shows that both are having different binding pose where only methyldithiocarbamate groups are overlapped. Derivative **8g** is below that of **13g** and which is persistent to all the remaining compounds in both the series. Also it is observed that the series with 9-H substitution having distinct binding pose than the co-crystallized ligand. Hence, 9-H substituted derivatives having different binding pose from 9-methyl substituted derivatives and co-crystallized ligand, therefore methyl group assist to keep this binding pose like co-crystal ligand. Deviation of this binding pose may be accountable for overall decrease in the biological activity of 9-H substituted derivatives. Moreover, the most active derivative **13g** having trifluoromethyl group and that fluorine is having orthogonal multipolar interactions with the carbonyl oxygen of Asn150 which may be responsible for the highest activity of **13g**. Additionally, the docking studies were also performed for the amine intermediates **7a–d** and **12a–d** and these results are showing different binding poses in compare to the final molecules. However, these intermediates (**7a–d** and **12a–d**) were lacking the two additional hydrogen bonding interactions which were fulfilled by dithiocarbamate group in final derivatives and this could be the reason for lesser activity of these intermediates.

To know the binding mode of action for these new molecules, DNA docking studies were performed on two different DNA structures, first with already intercalated co-crystal ligand (PDB ID 1NAB)[48] and second with co-crystallized ligand that binds in the minor groove of DNA (PDB ID 195D).[49] Docking studies on the 1NAB showed that these molecules bind properly at the

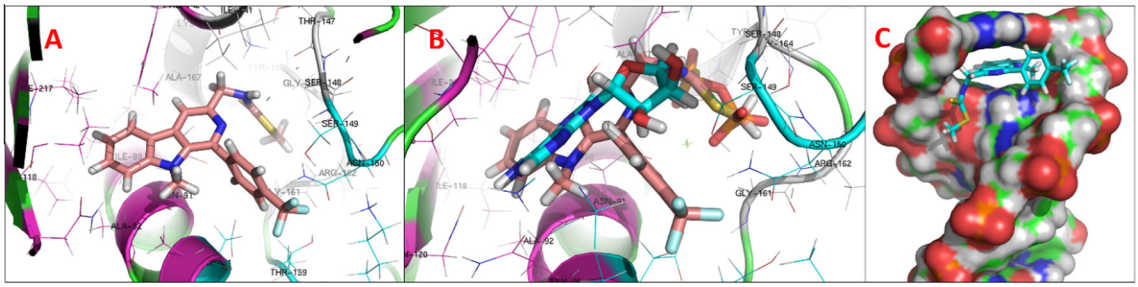

Figure 6. Docking poses for **13g**; (A) binding pose in topo II; (B) superimposed pose of **13g** and co-crystal ligand in topo II; (C) binding pose of **13g** in CT-DNA showing intercalation as binding mode.

intercalation site, whereas trifluoromethylphenyl and methyldithiocarbamate were extended out to the minor groove site and β-carboline ring stacks with the nucleotide base pairs, and NH of methyldithiocarbamate group shows strong hydrogen-bonding interactions with the carbonyl oxygen of cytosine. While docking studies on 195D showed that these molecules have potential to bind in the minor groove where β-carboline ring and methyldithiocarbamate groups are towards the minor groove and 4-trifluoromethylphenyl group extends out from the minor groove. Whereas in NH group of the methyldithiocarbamate forms additional hydrogen bonding interactions with sugar moiety of the nucleotide. Docking studies have shown that these molecules having potential for multiple modes of binding.

3. Conclusions

In conclusion, we have designed and synthesized a new class of dithiocarbamate linked β-carboline derivatives by introducing a substitution of the phenyl at the position-1, dithiocarbamate at position-3 and a H/methyl group at the position-9. These derivatives that contain two pharmacophoric groups such as β-carboline ring, dithiocarbamate and the derivatives **8j** and **13g** displayed promising cytotoxic activity and induced apoptosis. In addition, these derivatives also inhibit topo II enzymatic activity. However, the binding mode of both these derivatives with DNA is combilexin-type, which is different from the usual β-carboline alkaloids. Although both the derivatives exhibit good interaction with DNA, however the interaction of **8j** is better with DNA due to its planar structure. Perhaps, due to the influence of pharmacophores on the β-carboline ring, **13g** scored higher potential in cell biology studies. Nevertheless, these studies are useful for understanding the role of different pharmacophores that are connected to β-carboline nucleus in enhancing cytotoxicity, apoptosis, DNA binding ability and inhibition of DNA topo II.

4. Experimental section

4.1. Materials and methods

Chemistry: Chemical reagents were purchased from Sigma–Aldrich and were used without further purification. Anhydrous THF, CH_2Cl_2, CH_3CN, toluene, DMF and ether used in reactions were prepared by distillation under nitrogen over Na/benzophenone, CaH_2, Na/P_2O_5, and CaH_2/molecular sieves, respectively. Solvents for extraction and column chromatography were distilled prior to use. TLC analysis were performed with silica gel plates (0.25 mm, E. Merck, 60 F254) using ninhydrin, *p*-anisaldehyde, $KMnO_4$, iodine, and UV lamp for visualization. ^1H and ^{13}C NMR experiments were performed on 300 or 500 and 75 or 125 MHz, respectively, on a Bruker Avance. Chemical shifts are reported in parts per million (ppm) downstream from the internal tetramethylsilane standard. Spin multiplicities are described as s (singlet), br s (broad singlet), d (doublet), dd (double doublet), t (triplet), q (quartet) and m (multiplet). Coupling constants are reported in Hertz (Hz). Melting points were determined on an Electrothermal melting point apparatus and are uncorrected. FT-IR spectra for all compounds were recorded using thin film as well as a KBr pellet. Mass spectra were recorded by electrospray ionization mass spectrometry (ESI MS). High-resolution mass spectra (HRMS) were recorded on a QSTAR XL Derivative MS–MS mass spectrometer.

4.2. (*S*)-Methyl 2-amino-3-(1*H*-indol-3-yl)propanoate (2)[19]

To the stirred solution of L-tryptophan (0.1 mol) in methanol (50 ml), thionyl chloride 8.02 ml (0.11 mol) was added drop wise at 0 °C and continued stirring for 12 h at room temperature. Then, the excess amount of solvent was removed under vacuum and the crude product was azeotroped with toluene (2 × 10 ml) to obtain dry solid. Then, the resulting solid was dissolved in CH_2Cl_2, basified with saturated $NaHCO_3$ solution and extracted with excess amount of CH_2Cl_2. Then, the organic layer was dried over anhydrous sodium sulfate and concentrated under reduced pressure to obtain pure product. White solid; 19.62 g; 90% yield; mp: 102–103 °C; ^1H NMR (300 MHz, $CDCl_3$): δ 2.00 (s, 2H), 3.00 (dd, J = 4.12, 13.8 Hz, 1H), 3.25 (dd, J = 4.45, 13.8 Hz, 1H), 3.73 (s, 3H), 3.84 (t, J = 4.90, 5.42 Hz, 1H), 6.90 (s, 1H), 7.08 (t, J = 6.90, 7.14 Hz, 1H), 7.14 (t, J = 6.90, 7.14 Hz, 1H), 7.25 (d, J = 7.90 Hz, 1H), 7.58 (d, J = 7.90 Hz, 1H), 8.81 (br s, 1H); MS (ESI): m/z 219 $[M+H]^+$.

4.3. General reaction procedure for the preparation of compounds (4a–d)

To the mixture of L-tryptophan ester (**2**, 1 mmol) and substituted benzaldehyde (1.1 mmol) in ethanol, catalytic amount of *p*-TSA was added and the mixture was refluxed for 12 h. After completion of the reaction, ethanol was removed under vacuum and the resulting crude product **3a–d** (1.0 mmol) was taken in DMF and added triethylamine (3.0 mmol), a solution of trichloroisocyanuric acid (1.1 mmol) in DMF was added dropwise at −20 °C. The reaction mixture was slowly warmed up to 0 °C and stirred at this temperature for 2 h. After the completion of the reaction, added ice water, the resulted precipitate was filtered, washed with water, and dried under vacuum to give the compound (**4a–d**).

4.3.1. Methyl 1-(3,4,5-trimethoxyphenyl)-9*H*-pyrido[3,4-*b*]-indole-3-carboxylate (4a)[23]

Yellow solid: 76% yield; mp: 229–230 °C; ^1H NMR (300 MHz, $CDCl_3$) δ (ppm): 9.38 (br s, 1H), 8.75 (s, 1H), 8.21(d, J = 7.5 Hz, 1H), 7.60 (d, J = 7.5 Hz, 1H), 7.56–7.61 (m, 1H), 7.32–7.38 (m, 1H), 6.94 (s, 2H), 4.03 (s, 3H), 3.84 (s, 3H), 3.77 (s, 6H); ^{13}C NMR (75 MHz, DMSO-d_6 + $CDCl_3$) δ (ppm): 165.8, 152.7, 142.1, 141.2, 137.8, 136.1, 134.4, 132.8, 128.7, 128.0, 121.1, 120.9, 119.9, 116.1, 112.4, 105.5, 59.8, 55.5, 51.6; MS (ESI): m/z 393 $[M+H]^+$;

HRMS calculated for $C_{22}H_{21}O_5N_2$ *m/z* 393.14450 $[M+H]^+$, found *m/z* 393.14320.

4.3.2. Methyl 1-(4-methoxyphenyl)-9*H*-pyrido[3,4-*b*]indole-3-carboxylate (4b)[23]

White solid; 85% yield; mp: 226–230 °C; ^{1}H NMR (300 MHz, $CDCl_3$) δ (ppm): 9.18 (br s, 1H), 8.80 (s, 1H), 8.17 (d, *J* = 7.7 Hz, 1H), 7.78 (d, *J* = 8.8 Hz, 2H), 7.57–7.55 (m, 2H), 7.36–7.33 (m, 1H), 6.88 (d, *J* = 8.6 Hz, 2H), 4.03 (s, 3H), 3.77 (s, 3H); ^{13}C NMR (75 MHz, DMSO-d_6 + $CDCl_3$) δ (ppm): 165.9, 159.5, 141.9, 141.2, 136.2, 134.3, 129.9, 129.6, 128.6, 127.8, 121.0, 120.9, 119.8, 115.6, 113.5, 112.4, 54.8, 51.6; MS (ESI): *m/z* 333 $[M+H]^+$; HRMS calculated for $C_{20}H_{17}O_3N_2$ *m/z* 333.12337 $[M+H]^+$, found *m/z* 333.12194.

4.3.3. Methyl 1-(4-(trifluoromethyl)phenyl)-9*H*-pyrido[3,4-*b*]indole-3-carboxylate (4c)[23]

Pale yellow solid; 75% yield; mp: 250–252 °C; ^{1}H NMR (300 MHz, DMSO-d_6) δ (ppm): 11.99 (br s, 1H), 8.93 (s, 1H), 8.36 (d, *J* = 7.7 Hz, 1H), 8.23 (d, *J* = 7.7 Hz, 2H), 7.92 (d, *J* = 8.1 Hz, 2H), 7.68 (d, *J* = 8.1 Hz, 1H), 7.59 (t, *J* = 7.9 Hz, 1H), 7.32 (t, *J* = 7.5 Hz, 1H), 3.94 (s, 3H); ^{13}C NMR (75 MHz, DMSO-d_6) δ (ppm): 165.8, 141.4, 141.2, 140.2, 136.6, 134.6, 129.6, 129.5, 129.4, 129.2, 128.8, 125.5 (q, *J* = 3.3 Hz), 122.0, 120.9, 120.5, 117.2, 112.6, 52.0; MS (ESI): *m/z* 371 $[M+H]^+$; HRMS calculated for $C_{20}H_{14}F_3O_2N_2$ *m/z* 371.33257 $[M+H]^+$, found *m/z* 371.09941.

4.3.4. Methyl 1-(4-fluorophenyl)-9*H*-pyrido[3,4-*b*]indole-3-carboxylate (4d)[23]

White solid: 70% yield; mp: 195–198 °C; ^{1}H NMR (500 MHz, $CDCl_3$) δ (ppm): 8.87 (s, 1H), 8.83 (br s, 1H), 8.22 (d, *J* = 7.8 Hz, 1H), 7.92 (q, *J* = 5.3, 8.7 Hz, 2H), 7.63–7.55 (m, 2H), 7.39 (t, *J* = 7.9 Hz, 1H), 7.22 (t, *J* = 8.7 Hz, 2H), 4.06 (s, 3H); ^{13}C NMR (75 MHz, $CDCl_3$) δ (ppm): 165.7, 160.7 and 164.0 (d, *J* = 247.0 Hz), 141.3, 140.8, 136.3, 134.3, 133.7, 130.4 (d, *J* = 8.2 Hz), 129.0, 128.2, 121.3, 120.9, 120.0, 116.2, 115.2 (d, *J* = 21.4 Hz), 112.4, 51.6; MS (ESI): *m/z* 321 $[M+H]^+$; HRMS calculated for $C_{19}H_{14}O_2N_2F$ *m/z* 321.10338 $[M+H]^+$, found *m/z* 321.10298.

4.4. General reaction procedure for the preparation of compounds (9a–d)

To a stirred solution of **4a–d** (1 mmol) in DMF was added 60% NaH in paraffin oil (4 mmol) at 0 °C and stirred for 15 min. Then, added methyl iodide (1.2 mmol) and the reaction mixture was stirred for 4 h and added ice cold water slowly, extracted with ethyl acetate, washed with water, dried over sodium sulfate and concentrated under reduced pressure to get *N*-methyl compounds **9a–d**. These products were directly used for next step without any further purification.

4.4.1. Methyl 9-methyl-1-(3,4,5-trimethoxyphenyl)-9*H*-pyrido[3,4-*b*]indole-3-carboxylate (9a)

Off white solid: 72% yield; mp: 195–198 °C; ^{1}H NMR (300 MHz, $CDCl_3$) δ (ppm): 8.93 (s, 1H), 8.26 (d, *J* = 7.8 Hz, 1H), 7.67 (t, *J* = 7.9 Hz, 1H), 7.49 (d, *J* = 8.4 Hz, 1H), 7.40 (t, *J* = 7.6 Hz, 1H), 6.85 (s, 2H), 4.04 (s, 3H), 3.92 (s, 3H), 3.90 (s, 6H), 3.55 (s, 3H); ^{13}C NMR (75 MHz, $CDCl_3$) δ (ppm): 166.7, 153.1, 143.6, 143.0, 138.4, 136.6, 136.2, 134.5, 129.8, 128.9, 121.6, 121.2, 120.8, 116.8, 110.0, 107.1, 60.7, 56.2, 52.6, 32.7; MS (ESI): *m/z* 407 $[M+H]^+$, HRMS calculated for $C_{23}H_{23}N_2O_5$ *m/z* 407.16015 $[M+H]^+$, found *m/z* 407.16019.

4.4.2. Methyl 1-(4-methoxyphenyl)-9-methyl-9*H*-pyrido[3,4-*b*]-indole-3-carboxylate (9b)

Cream white solid: 80% yield; mp: 210–215 °C; ^{1}H NMR (300 MHz, $CDCl_3$) δ (ppm): 8.88 (s, 1H), 8.24 (d, *J* = 7.8 Hz, 1H), 7.66–7.62 (m, 1H), 7.58 (d, *J* = 8.7 Hz, 2H), 7.46 (d, *J* = 8.4 Hz, 1H), 7.40–7.36 (m, 1H), 7.05 (d, *J* = 8.7 Hz, 2H), 4.03 (s, 3H), 3.90 (s, 3H), 3.51 (s, 3H); ^{13}C NMR (125 MHz, $CDCl_3$) δ (ppm): 166.8, 160.0, 143.8, 143.1, 136.8, 136.5, 131.5, 131.0, 129.8, 128.7, 121.6, 121.3, 120.7, 116.4, 113.6, 110.0, 55.3, 52.6, 32.9; MS (ESI): *m/z* 347 $[M+H]^+$, HRMS calculated for $C_{21}H_{19}N_2O_3$ *m/z* 347.13902 $[M+H]^+$, found *m/z* 347.13894.

4.4.3. Methyl 9-methyl-1-(4-(trifluoromethyl)phenyl)-9*H*-pyrido[3,4-*b*]indole-3-carboxylate (9c)

White solid: 73% yield; mp: 220–225 °C; ^{1}H NMR (300 MHz, $CDCl_3$) δ (ppm): 8.94 (s, 1H), 8.26 (d, *J* = 7.8 Hz, 1H), 7.80 (s, 4H), 7.68 (t, *J* = 7.9 Hz, 1H), 7.49 (d, *J* = 8.2 Hz, 1H), 7.41 (t, *J* = 7.9 Hz, 1H), 4.04 (s, 3H), 3.50 (s, 3H); ^{13}C NMR (75 MHz, $CDCl_3$) δ (ppm): 166.5, 143.1, 142.7, 142.0, 137.1, 136.3, 130.4, 130.3, 129.2, 125.8, 125.2 (q, *J* = 3.3 Hz), 122.2, 121.7, 121.2, 121.0, 117.1, 110.1, 52.7, 33.2; MS (ESI): *m/z* 385 $[M+H]^+$, HRMS calculated for $C_{21}H_{16}O_2N_2F_3$ *m/z* 385.11584 $[M+H]^+$, found *m/z* 385.11554.

4.4.4. Methyl 1-(4-fluorophenyl)-9-methyl-9*H*-pyrido[3,4-*b*]-indole-3-carboxylate (9d)

Cream white solid: 76% yield; mp: 223–225 °C; ^{1}H NMR (300 MHz, $CDCl_3$) δ (ppm): 8.91 (s, 1H), 8.25 (d, *J* = 7.8 Hz, 1H), 7.67–7.63 (m, 3H), 7.48 (d, *J* = 8.4 Hz, 1H), 7.40 (t, *J* = 7.2 Hz, 1H), 7.23 (t, *J* = 8.7 Hz, 2H), 4.04 (s, 3H), 3.50 (s, 3H); ^{13}C NMR (75 MHz, $CDCl_3$) δ (ppm): 166.6, 164.7 and 161.4 (d, *J* = 248.1 Hz), 143.1, 142.7, 136.9, 136.4, 135.2, 131.6 (d, *J* = 8.2 Hz), 130.1, 129.0, 121.7, 121.3, 120.9, 116.8, 115.3 (d, *J* = 22.0 Hz), 110.0, 52.7, 32.9; MS (ESI): *m/z* 335 $[M+H]^+$, HRMS calculated for $C_{20}H_{16}O_2N_2F$ *m/z* 335.11903 $[M+H]^+$, found *m/z* 335.11872.

4.5. General reaction procedure for the preparation of compounds (5a–d and 10a–d)

A stirred suspension of compounds **4a–d**/**9a–d** (20 mmol) in dry THF (60 mL) was added $LiBH_4$ (22 mmol) at 0 °C and stirred for 4 h at room temperature. Then, the reaction mixture was quenched with saturated NH_4Cl solution and extracted with ethyl acetate and washed with water. The organic layer was dried over anhydrous sodium sulfate and evaporated under reduced pressure. Then, the crude residue was used directly for the next step without any further purification.

4.6. General reaction procedure for the preparation of compounds (6a–d and 11a–d)

To a stirred solution of **5a–d**/**10a–d** (10 mmol) in dry THF was added DBU (15 mmol) and DPPA (12 mmol) at 0 °C. The reaction mixture was stirred for 16 h at rt and the reaction mixture was quenched with water, extracted with ethyl acetate and washed with water. The combined organic phases were dried over sodium sulfate and concentrated under reduced pressure to get crude products, which were purified by column chromatography using silica gel to get pure compounds **6a–d**/**11a–d**.

4.6.1. 3-(Azidomethyl)-1-(3,4,5-trimethoxyphenyl)-9*H*-pyrido[3,4-*b*]indole (6a)

Light yellow solid: 75% yield mp: 130–135 °C; ^{1}H NMR (300 MHz, $CDCl_3$) δ (ppm): 8.75 (s, 1H), 8.16 (d, *J* = 7.8 Hz, 1H), 7.95 (s, 1H), 7.60–7.54 (m, 2H), 7.33 (t, *J* = 7.9 Hz, 1H), 7.18 (s, 2H), 4.66 (s, 2H), 3.93 (s, 6H), 3.92 (s, 3H); ^{13}C NMR (125 MHz, $CDCl_3$) δ (ppm): 153.9, 145.4, 142.6, 140.7, 138.8, 133.7, 132.8, 130.7, 128.7, 121.8, 120.5, 112.3, 111.7, 105.6, 60.9, 56.4, 55.8; MS (ESI): *m/z* 390 $[M+H]^+$, HRMS calculated for $C_{21}H_{20}O_3N_5$ *m/z* 390.15607 $[M+H]^+$, found *m/z* 390.15609.

4.6.2. 3-(Azidomethyl)-1-(4-methoxyphenyl)-9*H*-pyrido[3,4-*b*]indole (6b)

Yellow solid: 80% yield; mp: 134–136 °C; ^{1}H NMR (300 MHz, $CDCl_3$) δ (ppm): 8.50 (s, 1H), 8.15 (d, J = 7.8 Hz, 1H), 7.95–7.92 (m, 3H), 7.58–7.54 (m, 1H), 7.51 (d, J = 8.0 Hz, 1H), 7.32 (t, J = 7.2 Hz, 1H), 7.12 (d, J = 8.7 Hz, 2H), 4.68 (s, 2H), 3.90 (s, 3H); ^{13}C NMR (125 MHz, $CDCl_3$) δ (ppm): 160.2, 145.2, 142.5, 140.6, 132.6, 130.6, 130.5, 129.4, 128.5, 121.8, 121.7, 120.3, 114.6, 111.8, 111.5, 56.1, 55.4; MS (ESI): m/z 330 $[M+H]^+$, HRMS calculated for $C_{19}H_{16}ON_5$ m/z 330.13494 $[M+H]^+$, found m/z 330.13530.

4.6.3. 3-(Azidomethyl)-1-(4-(trifluoromethyl)phenyl)-9*H*-pyrido[3,4-*b*]indole (6c)

Yellow solid: 68% yield; mp: 138–140 °C; ^{1}H NMR (300 MHz, $CDCl_3$) δ (ppm): 8.49 (s, 1H), 8.17 (d, J = 7.9 Hz, 1H), 8.11 (d, J = 7.9 Hz, 2H), 8.01 (s, 1H), 7.84 (d, J = 8.0 Hz, 2H), 7.61–7.57 (m, 1H), 7.52 (d, J = 8.2 Hz, 1H), 7.37–7.33 (m, 1H), 4.69 (s, 2H); ^{13}C NMR (125 MHz, $CDCl_3$) δ (ppm): 145.6, 141.5, 140.7, 132.8, 131.2, 130.9, 130.6, 129.0, 128.4, 126.1 (q, J = 3.6 Hz), 125.0, 121.8, 121.6, 120.7, 113.0, 111.6, 55.9; MS (ESI): m/z 368 $[M+H]^+$, HRMS calculated for $C_{19}H_{13}N_5F_3$ m/z 368.11176 $[M+H]^+$, found m/z 368.11170.

4.6.4. 3-(Azidomethyl)-1-(4-fluorophenyl)-9*H*-pyrido[3,4-*b*]indole (6d)

Cream white solid: 86% yield; mp: 140–143 °C; ^{1}H NMR (300 MHz, $CDCl_3$) δ (ppm): 8.46 (s, 1H), 8.15 (d, J = 7.7 Hz, 1H), 7.99–7.93 (m, 3H), 7.61–7.48 (m, 2H), 7.36–7.23 (m, 3H), 4.67 (s, 2H); ^{13}C NMR (125 MHz, $CDCl_3$) δ (ppm): 164.1 and 162.1 (d, J = 248.8 Hz), 145.3, 141.5, 140.6, 134.2, 132.7, 130.8, 129.9 (d, J = 8.2 Hz), 128.7, 121.8, 121.7, 120.5, 116.2 (d, J = 21.8 Hz), 112.4, 111.6, 56.0; MS (ESI): m/z 318 $[M+H]^+$, HRMS calculated for $C_{18}H_{13}N_5F$ m/z 318.11495 $[M+H]^+$, found m/z 318.11458.

4.6.5. 3-(Azidomethyl)-9-methyl-1-(3,4,5-trimethoxyphenyl)-9*H*-pyrido[3,4-*b*]indole (11a)

Light yellow solid: 85% yield; mp: 128–132 °C; ^{1}H NMR (300 MHz, $CDCl_3$) δ (ppm): 8.19 (d, J = 7.8 Hz, 1H), 8.03 (s, 1H), 7.64 (t, J = 7.6 Hz, 1H), 7.45 (d, J = 8.4 Hz, 1H), 7.34 (t, J = 7.5 Hz, 1H), 6.8 (s, 2H), 4.69 (s, 2H), 3.93 (s, 3H), 3.91 (s, 6H), 3.55 (s, 3H); ^{13}C NMR (125 MHz, $CDCl_3$) δ (ppm): 153.1, 143.9, 143.6, 143.2, 138.2, 134.8, 134.3, 130.9, 128.7, 121.5, 120.9, 120.0, 112.2, 109.8, 106.8, 60.9, 56.1, 55.8, 32.8; MS (ESI): m/z 404 $[M+H]^+$, HRMS calculated for $C_{22}H_{22}O_3N_5$ m/z 404.17172 $[M+H]^+$, found m/z 404.17199.

4.6.6. 3-(Azidomethyl)-1-(4-methoxyphenyl)-9-methyl-9*H*-pyrido[3,4-*b*]indole (11b)

Light yellow solid: 78% yield; mp: 120–125 °C; ^{1}H NMR (300 MHz, $CDCl_3$) δ (ppm): 8.18 (d, J = 7.9 Hz, 1H), 7.99 (s, 1H), 7.63–7.60 (m, 1H), 7.59 (d, J = 8.7 Hz, 2H), 7.43 (d, J = 8.2 Hz, 1H), 7.34–7.30 (m, 1H), 7.06 (d, J = 8.7 Hz, 2H), 4.68 (s, 2H), 3.90 (s, 3H), 3.50 (s, 3H); ^{13}C NMR (125 MHz, $CDCl_3$) δ (ppm): 159.9, 144.0, 143.7, 143.3, 134.6, 131.9, 130.8, 128.5, 121.5, 121.0, 119.9, 113.7, 111.8, 109.8, 56.0, 55.4, 32.9; MS (ESI): m/z 344 $[M+H]^+$, HRMS calculated for $C_{20}H_{18}ON_5$ m/z 344.15059 $[M+H]^+$, found m/z 344.15067.

4.6.7. 3-(Azidomethyl)-9-methyl-1-(4-(trifluoromethyl)phenyl)-9*H*-pyrido[3,4-*b*]indole (11c)

Yellow solid: 67% yield; mp: 120–123 °C; ^{1}H NMR (300 MHz, $CDCl_3$) δ (ppm): 8.20 (d, J = 7.8 Hz, 1H), 8.06 (s, 1H), 7.80 (s, 4H), 7.66–7.62 (m, 1H), 7.45 (d, J = 8.4 Hz, 1H), 7.37–7.33 (m, 1H), 4.69 (s, 2H), 3.48 (s, 3H); ^{13}C NMR (125 MHz, $CDCl_3$) δ (ppm): 144.3, 143.3, 143.0, 141.9, 134.4, 131.4, 130.7, 130.4, 130.0, 129.0, 125.2 (q, J = 3.6 Hz), 121.6, 120.9, 120.3, 112.7, 109.9, 55.8, 33.2; MS (ESI): m/z 382 $[M+H]^+$, HRMS calculated for $C_{20}H_{15}N_5F_3$ m/z 382.12741 $[M+H]^+$, found m/z 382.12788.

4.6.8. 3-(Azidomethyl)-1-(4-fluorophenyl)-9-methyl-9*H*-pyrido[3,4-*b*]indole (11d)

Light yellow solid: 83% yield; mp: 140–143 °C; ^{1}H NMR (300 MHz, $CDCl_3$) δ (ppm): 8.19 (d, J = 7.7 Hz, 1H), 8.03 (s, 1H), 7.67–7.59 (m, 3H), 7.44 (d, J = 8.3 Hz, 1H), 7.33 (t, J = 7.5 Hz, 1H), 7.25–7.19 (m, 2H), 4.68 (s, 2H), 3.48 (s, 3H); ^{13}C NMR (125 MHz, $CDCl_3$) δ (ppm): 163.9 and 162.0 (d, J = 247.9 Hz), 144.1, 143.3, 142.6, 135.5, 134.5, 131.4 (d, J = 8.2 Hz), 131.1, 128.7, 121.5, 120.9, 120.1, 115.3 (d, J = 21.8 Hz), 112.2, 109.8, 55.9, 32.9; MS (ESI): m/z 332 $[M+H]^+$, HRMS calculated for $C_{19}H_{15}N_5F$ m/z 332.13060 $[M+H]^+$, found m/z 332.13056.

4.7. General reaction procedure for the preparation of compounds (7a–d and 12a–d)

To a stirred solution of azide compounds **6a–d**/**11a–d** (1 mmol) in acetonitrile and water (1:1) was added triphenylphosphene (1.1 mmol) and stirred for 12 h at rt. The solvent was removed in vacuo, to this residue was added 6 N HCl solution and washed with ethyl acetate to remove non basic impurities. Then separated acidic medium and basified with 20% NaOH solution (up to pH = 10), extracted with chloroform, washed with water, dried over sodium sulfate and concentrated under reduced pressure to get crude amine products which were triturated in 10% ethyl acetate/hexane, decanted and dried to get pure amine products (**7a–d**/**12a–d**).

4.7.1. (1-(3,4,5-Trimethoxyphenyl)-9*H*-pyrido[3,4-*b*]indol-3-yl)methanamine (7a)

Cream white solid: 68% yield; mp: 140–145 °C; ^{1}H NMR (300 MHz, $CDCl_3$) δ (ppm): 8.65 (s, 1H), 8.14 (d, J = 7.8 Hz, 1H), 7.90 (s, 1H), 7.57–7.50 (m, 2H), 7.30 (t, J = 7.8 Hz, 1H), 7.13 (s, 2H), 4.19 (s, 2H), 3.94 (s, 6H), 3.92 (s, 3H); ^{13}C NMR (125 MHz, $CDCl_3$) δ (ppm): 153.7, 148.6, 142.3, 140.8, 138.4, 134.0, 132.5, 130.6, 128.4, 121.7, 120.0, 112.3, 111.6, 111.1, 105.5, 60.8, 56.3, 47.3; MS (ESI): m/z 364 $[M+H]^+$, HRMS calculated for $C_{21}H_{22}O_3N_3$ m/z 364.16557 $[M+H]^+$, found m/z 364.16557.

4.7.2. (1-(4-Methoxyphenyl)-9*H*-pyrido[3,4-*b*]indol-3-yl)methanamine (7b)

Cream white solid: 70% yield; mp: 170–173 °C; ^{1}H NMR (300 MHz, $CDCl_3$) δ (ppm): 8.49 (s, 1H), 8.13 (d, J = 7.9 Hz, 1H), 7.92 (d, J = 8.8 Hz, 2H), 7.86 (s, 1H), 7.55–7.51 (m, 1H), 7.48 (d, J = 8.2 Hz, 1H), 7.31–7.27 (m, 1H), 7.12 (d, J = 8.7 Hz, 2H), 4.18 (s, 2H), 3.90 (s, 3H); ^{13}C NMR (75 MHz, $CDCl_3$ + DMSO-d_6) δ (ppm): 159.4, 150.4, 141.6, 141.1, 132.1, 130.9, 130.0, 129.3, 127.5, 121.1, 120.9, 119.0, 113.8, 111.6, 109.8, 54.9, 47.5; MS (ESI): m/z 304 $[M+H]^+$, HRMS calculated for $C_{19}H_{18}ON_3$ m/z 304.14444 $[M+H]^+$, found m/z 304.14414.

4.7.3. (1-(4-(Trifluoromethyl)phenyl)-9*H*-pyrido[3,4-*b*]indol-3-yl)methanamine (7c)

Cream white solid: 78% yield; mp: 210–213 °C; ^{1}H NMR (300 MHz, $CDCl_3$) δ (ppm): 8.77 (s, 1H), 8.11 (d, J = 7.9 Hz, 1H), 8.02 (d, J = 8.1 Hz, 2H), 7.90 (s, 1H), 7.81 (d, J = 8.1 Hz, 2H), 7.57–7.53 (m, 1H), 7.48 (d, J = 8.2 Hz, 1H), 7.32–7.28 (m, 1H), 4.17 (s, 2H); ^{13}C NMR (75 MHz, $CDCl_3$ + DMSO-d_6) δ (ppm): 150.9, 142.1, 141.4, 139.9, 132.5, 130.8, 127.8, 128.0, 125.7, 125.3 (q, J = 3.3 Hz), 122.1, 121.2, 121.1, 119.4, 111.8, 111.2, 47.7; MS (ESI): m/z 342 $[M+H]^+$, HRMS calculated for $C_{19}H_{15}N_3F_3$ m/z 342.12126 $[M+H]^+$, found m/z 342.12124.

4.7.4. (1-(4-Fluorophenyl)-9*H*-pyrido[3,4-*b*]indol-3-yl)methanamine (7d)

Cream white solid: 66% yield; mp: 190–195 °C; ^{1}H NMR (300 MHz, $CDCl_3$) δ (ppm): 8.54 (s, 1H), 8.13 (d, J = 7.9 Hz, 1H), 7.96 (q, J = 5.3, 8.5 Hz, 2H), 7.90 (s, 1H), 7.54 (t, J = 8.1 Hz, 1H), 7.49 (d, J = 8.2 Hz, 1H), 7.32–7.25 (m, 3H), 4.18 (s, 2H); ^{13}C NMR (75 MHz, $CDCl_3$ + DMSO-d_6) δ (ppm): 162.8 and 159.6 (d, J = 247.0 Hz), 149.6, 140.4, 139.1, 133.6, 130.9, 129.2 (d, J = 7.1 Hz), 129.1, 126.6, 119.9, 119.8, 118.0, 114.2 (d, J = 21.4 Hz), 110.9, 109.2, 46.5; MS (ESI): m/z 292 $[M+H]^+$, HRMS calculated for $C_{18}H_{15}N_3F$ m/z 292.12445 $[M+H]^+$, found m/z 292.12400.

4.7.5. (9-Methyl-1-(3,4,5-trimethoxyphenyl)-9*H*-pyrido[3,4-*b*]-indol-3-yl)methanamine (12a)

Light yellow solid: 80% yield; mp: 125–130 °C; ^{1}H NMR (300 MHz, $CDCl_3$) δ (ppm): 8.17 (d, J = 7.7 Hz, 1H), 8.00 (s, 1H), 7.61 (t, J = 7.7 Hz, 1H), 7.42 (d, J = 8.3 Hz, 1H), 7.31 (t, J = 7.4 Hz, 1H), 6.85 (s, 2H), 4.20 (s, 2H), 3.93 (s, 3H), 3.91 (s, 6H), 3.50 (s, 3H); ^{13}C NMR (125 MHz, $CDCl_3$) δ (ppm): 153.0, 143.3, 142.2, 138.2, 131.0, 128.6, 128.3, 121.5, 119.8, 119.6, 112.1, 111.2, 109.7, 106.9, 106.8, 66.6, 60.9, 56.2, 32.6; MS (ESI): m/z 378 $[M+H]^+$, HRMS calculated for $C_{22}H_{24}O_3N_3$ m/z 378.18122 $[M+H]^+$, found m/z 378.18221.

4.7.6. (1-(4-Methoxyphenyl)-9-methyl-9*H*-pyrido[3,4-*b*]indol-3-yl)methanamine (12b)

Cream white solid: 75% yield; mp: 120–125 °C; ^{1}H NMR (300 MHz, $CDCl_3$) δ (ppm): 8.16 (d, J = 7.8 Hz, 1H), 7.94 (s, 1H), 7.61–7.56 (m, 3H), 7.41 (d, J = 8.2 Hz, 1H), 7.29 (t, J = 7.8 Hz, 1H), 7.05 (d, J = 8.7 Hz, 2H), 4.17 (s, 2H), 3.90 (s, 3H), 3.47 (s, 3H); ^{13}C NMR (125 MHz, $CDCl_3$) δ (ppm): 159.7, 150.6, 143.3, 143.2, 134.1, 132.3, 132.0, 130.8, 128.2, 121.4, 121.1, 119.5, 113.5, 110.4, 109.6, 55.3, 48.0, 32.7; MS (ESI): m/z 318 $[M+H]^+$, HRMS calculated for $C_{20}H_{20}ON_3$ m/z 318.16009 $[M+H]^+$, found m/z 318.16033.

4.7.7. (9-Methyl-1-(4-(trifluoromethyl)phenyl)-9*H*-pyrido[3,4-*b*]-indol-3-yl)methanamine (12c)

Cream white solid: 68% yield; mp: 125–130 °C; ^{1}H NMR (300 MHz, $CDCl_3$) δ (ppm): 8.18 (d, J = 7.7 Hz, 1H), 8.02 (s, 1H), 7.80 (s, 4H), 7.65–7.59 (m, 1H), 7.42 (d, J = 7.9 Hz, 1H), 7.32 (t, J = 7.7 Hz, 1H), 4.20 (s, 2H), 3.46 (s, 3H); ^{13}C NMR (125 MHz, $CDCl_3$) δ (ppm): 150.8, 143.5, 143.3, 141.5, 134.1, 131.3, 130.5, 130.0, 128.6, 125.1 (q, J = 3.7), 123.0, 121.5, 121.0, 119.9, 111.3, 109.7, 47.8, 33.1; MS (ESI): m/z 356 $[M+H]^+$, HRMS calculated for $C_{20}H_{17}N_3F_3$ m/z 356.13691 $[M+H]^+$, found m/z 356.13739.

4.7.8. (1-(4-Fluorophenyl)-9-methyl-9*H*-pyrido[3,4-*b*]indol-3-yl)methanamine (12d)

Cream white solid mp: 127–130 °C; ^{1}H NMR (300 MHz, $CDCl_3$) δ (ppm): 8.1 (d, J = 7.8 Hz, 1H), 7.97 (s, 1H), 7.64–7.59 (m, 3H), 7.41 (d, J = 8.2 Hz, 1H), 7.30 (t, J = 7.9 Hz, 1H), 7.22 (t, J = 8.7 Hz, 2H), 4.18 (s, 2H), 3.44 (s, 3H); ^{13}C NMR (125 MHz, $CDCl_3$) δ (ppm): 163.8 and 161.8 (d, J = 247.9 Hz), 150.5, 143.3, 142.2, 135.9, 134.1, 132.0, 131.4 (d, J = 8.2 Hz), 128.4, 121.4, 121.0, 119.7, 115.2 (d, J = 20.8 Hz), 110.9, 109.6, 47.8, 32.8; MS (ESI): m/z 306 $[M+H]^+$, HRMS calculated for $C_{19}H_{17}N_3F$ m/z 306.14010 $[M+H]^+$, found m/z 306.14041.

4.8. General reaction procedure for the preparation of compounds (8a–l and 13a–l)

To a stirred solution of amine compounds **7a–d**/**12a–d** (1 mmol) in pyridine (1 ml) was added TEA (1.3 mmol) and carbon disulfide (1.5 mmol) at 0 °C and stirred for 15 min. Then, to this reaction mixture was added alkyl bromide (1.1 mmol) and reaction mixture was stirred at 0 °C for 30 min. The reaction mixture was quenched with water, extracted with chloroform, washed with water, dried over sodium sulfate and concentrated under reduced pressure to get crude product. The crude product was purified by silica gel column chromatography by using ethyl acetate/hexane.

4.8.1. Methyl ((1-(3,4,5-trimethoxyphenyl)-9*H*-pyrido[3,4-*b*]-indol-3-yl)methyl)carbamodithioate (8a)

Light green solid: 86% yield; mp: 197–198 °C; ^{1}H NMR (300 MHz, CD_6CO) δ (ppm): 10.77 (s, 1H), 9.59 (br s, 1H), 8.25 (d, J = 8.1 Hz, 1H), 8.10 (s, 0.9H), 7.68–7.52 (m, 2H), 7.30–7.25 (m, 3H), 5.20 (s, 1.8H), 3.94 (s, 6H), 3.83 (s, 3H), 2.65 (s, 3H) and peaks at 8.02 and 5.00 are due to 10% minor rotamer; ^{13}C NMR (75 MHz, CD_6CO) δ (ppm): 199.7, 155.5, 146.3, 143.7, 143.6, 135.7, 134.6, 132.5, 130.2, 123.4, 123.3, 121.6, 114.1, 113.6, 113.3, 107.7, 61.6, 57.4, 53.7, 18.9; FT-IR: 3299.85, 3147.58, 2961.84, 2910.37, 1624.14, 1585.03, 1501.36, 1389.10, 1233.81 cm^{-1}; MS (ESI): m/z 454 $[M+H]^+$, HRMS calculated for $C_{23}H_{24}O_3N_3S_2$ m/z 454.12536 $[M+H]^+$, found m/z 454.12516.

4.8.2. Allyl ((1-(3,4,5-trimethoxyphenyl)-9*H*-pyrido[3,4-*b*]indol-3-yl)methyl)carbamodithioate (8b)

Off white solid: 78% yield; mp: 195–197 °C; ^{1}H NMR (300 MHz, DMSO-d_6) δ (ppm): 11.53 (s, 1H), 10.53 (bt, J = 5.1 Hz, 1H), 8.22 (d, J = 7.7 Hz, 1H), 8.00 (s, 1H), 7.65–7.51 (m, 2H), 7.30–7.22 (m, 3H), 5.97–5.82 (m, 1H), 5.30 (d, J = 16.9 Hz, 1H), 5.15–5.08 (m, 3H), 3.95 (d, J = 8.1 Hz, 2H), 3.92 (s, 6H), 3.77 (s, 3H) and peaks at 10.63, 4.88 and 4.02 are due to 10% minor rotamer; ^{13}C NMR (75 MHz, CD_6CO) δ (ppm): 195.5, 153.0, 144.5, 141.5, 141.4, 137.9, 133.4, 132.1, 129.9, 128.3, 121.5, 120.7, 119.6, 118.1, 112.5, 111.7, 105.8, 60.1, 55.8, 51.8, 37.0; FT-IR: 3297.48, 3134.44, 2971.05, 2920.87, 1623.77, 1504.51, 1470.65, 1387.38, 1231.35 cm^{-1}; MS (ESI): m/z 480 $[M+H]^+$, HRMS calculated for $C_{25}H_{26}O_3N_3S_2$ m/z 480.14101 $[M+H]^+$, found m/z 480.13983.

4.8.3. Benzyl ((1-(3,4,5-trimethoxyphenyl)-9*H*-pyrido[3,4-*b*]-indol-3-yl)methyl)carbamodithioate (8c)

Cream color solid: 80% yield; mp: 155–160 °C; ^{1}H NMR (300 MHz, DMSO-d_6) δ (ppm): 11.53 (s, 1H), 10.57 (bt, J = 5.3 Hz, 0.9H), 8.21 (d, J = 7.7 Hz, 1H), 8.00 (s, 1H), 7.68–7.49 (m, 2H), 7.43–7.36 (m, 2H), 7.34–7.21 (m, 6H), 5.13 (d, J = 5.3 Hz, 1.8H), 4.56 (s, 2H), 3.90 (s, 6H), 3.77 (s, 3H) and peaks at 10.66 and 4.88 are due to 10% minor rotamer; ^{13}C NMR (125 MHz, $CDCl_3$) δ (ppm): 196.4, 153.7, 143.4, 141.7, 141.1, 138.7, 136.5, 133.4, 132.8, 131.1, 129.0, 128.9, 128.5, 127.4, 121.9, 121.5, 120.5, 112.1, 111.8, 105.4, 60.9, 56.3, 51.7, 39.8; FT-IR: 3321.70, 3129.08, 2932.96, 1625.07, 1584.30, 1496.18, 1453.10, 1389.25, 1234.75, 1127.46 cm^{-1}; MS (ESI): m/z 530 $[M+H]^+$, HRMS calculated for $C_{29}H_{28}O_3N_3S_2$ m/z 530.15666 $[M+H]^+$, found m/z 530.15701.

4.8.4. Methyl ((1-(4-methoxyphenyl)-9*H*-pyrido[3,4-*b*]indol-3-yl)methyl)carbamodithioate (8d)

Off white solid: 85% yield; mp: 197–200 °C; ^{1}H NMR (300 MHz, DMSO-d_6) δ (ppm): 11.04 (s, 1H), 9.95 (s, 1H), 8.04 (d, J = 7.9 Hz, 1H), 7.94 (d, J = 8.7 Hz, 2H), 7.83 (s, 1H), 7.55 (d, J = 8.1 Hz, 1H), 7.43 (t, J = 7.4 Hz, 1H), 7.15 (t, J = 7.5 Hz, 1H), 7.04 (d, J = 8.5 Hz, 2H), 5.10 (d, J = 4.9 Hz, 1.8H), 3.84 (s, 3H), 2.57 (s, 3H) and peak at 4.86 is due to 10% minor rotamer; ^{13}C NMR (125 MHz, $CDCl_3$ + DMSO-d_6) δ (ppm): 197.6, 159.5, 144.3, 141.4, 141.2, 131.9, 130.4, 129.8, 129.6, 127.7, 121.0, 120.6, 119.1, 113.8, 112.2, 110.8, 55.0, 51.8, 17.4; FT-IR: 3295.41, 3236.34, 2923.86, 1739.36, 1575.92, 1624.78, 1489.43, 1437.74, 1247.16, 1232.27, 1175.75 cm^{-1}; MS (ESI): m/z 394 $[M+H]^+$, HRMS calculated for $C_{21}H_{20}ON_3S_2$ m/z 394.10423 $[M+H]^+$, found m/z 394.10425.

4.8.5. Allyl ((1-(4-methoxyphenyl)-9*H*-pyrido[3,4-*b*]indol-3-yl)methyl)carbamodithioate (8e)

Cream color solid: 78% yield; mp: 170–175 °C; ^{1}H NMR (300 MHz, $CDCl_3$) δ (ppm): 8.88 (br s, 0.9H), 8.50 (s, 1H), 8.12 (d, J = 7.7 Hz, 1H), 7.89 (d, J = 8.5 Hz, 2H), 7.85 (s, 0.9H), 7.60–7.48 (m, 2H), 7.31 (t, J = 7.5 Hz, 1H), 7.12 (d, J = 8.5 Hz, 2H), 6.05–5.85 (m, 1H), 5.30 (d, J = 17.2 Hz, 1H), 5.16 (d, J = 4.2 Hz, 1.8H), 5.12 (d, J = 9.6 Hz, 1H), 3.96 (d, J = 6.8 Hz, 1.8H), 3.91 (s, 3H) and peaks at 8.98, 7.79, 4.92 and 4.10 is due to 10% minor rotamer; ^{13}C NMR (75 MHz, $CDCl_3$ + DMSO-d_6) δ (ppm): 195.4, 159.2, 142.7, 141.0, 140.8, 132.1, 131.9, 129.9, 129.8, 129.1, 127.5, 120.6, 120.4, 118.8, 117.4, 113.4, 111.6, 110.6, 54.6, 51.2, 37.2; FT-IR: 3244.40, 3058.12, 2951.63, 1739.00, 1625.31, 1607.56, 1490.25, 1439.96, 1320.20, 1234.54, 1182.23 cm^{-1}; MS (ESI): m/z 420 [M+H]$^+$, HRMS calculated for $C_{23}H_{22}ON_3S_2$ m/z 420.11988 [M+H]$^+$, found m/z 420.11971.

4.8.6. Benzyl ((1-(4-methoxyphenyl)-9*H*-pyrido[3,4-*b*]indol-3-yl)methyl)carbamodithioate (8f)

Light yellow solid: 82% yield; mp: 172–176 °C; ^{1}H NMR (500 MHz, $CDCl_3$) δ (ppm): 8.98 (br s, 1H), 8.64 (br s, 1H), 8.10 (d, J = 7.9 Hz, 1H), 7.88–7.83 (m, 3H), 7.58–7.49 (m, 2H), 7.38 (d, J = 7.3 Hz, 1.7H), 7.34–7.22 (m, 4H), 7.07 (d, J = 8.4 Hz, 2H), 5.17 (d, J = 3.9 Hz, 1.7H), 4.58 (s, 1.7H), 3.87 (s, 3H) and peak at 7.44, 4.88 and 4.68 are due to 15% minor rotamer; ^{13}C NMR (75 MHz, $CDCl_3$) δ (ppm): 196.2, 160.2, 143.1, 141.3, 140.9, 136.4, 132.5, 130.9, 129.3, 129.0, 128.8, 128.5, 127.3, 121.8, 121.7, 121.4, 120.4, 114.5, 111.6, 111.1, 55.4, 51.5, 39.8; FT-IR: 3300.56, 3030.98, 2970.36, 1738.88, 1625.65, 1606.60, 1490.34, 1441.79, 1352.69, 1230.64, 1181.26 cm^{-1}; MS (ESI): m/z 470 [M+H]$^+$, HRMS calculated for $C_{27}H_{24}ON_3S_2$ m/z 470.13553 [M+H]$^+$, found m/z 470.13538.

4.8.7. Methyl ((1-(4-(trifluoromethyl)phenyl)-9*H*-pyrido[3,4-*b*]-indol-3-yl)methyl)carbamodithioate (8g)

White solid: 80% yield; mp: 218–222 °C; ^{1}H NMR (500 MHz, $CDCl_3$) δ (ppm): 8.69 (br s, 0.9H), 8.45 (br s, 1H), 8.17 (d, J = 7.9 Hz, 1H), 8.10 (d, J = 8.1 Hz, 2H), 7.98 (s, 0.8H), 7.89 (d, J = 8.2 Hz, 2H), 7.60 (t, J = 8.1 Hz, 1H), 7.53 (d, J = 8.1 Hz, 1H), 7.35 (t, J = 7.8 Hz, 1H), 5.22 (d, J = 4.4 Hz, 1.7H), 2.69 (s, 2.5H) and peak at 8.90, 7.94, 4.97 and 2.76 are due to 15% minor rotamer; ^{13}C NMR (75 MHz, $CDCl_3$ + DMSO-d_6) δ (ppm): 197.4, 143.5, 141.2, 139.0, 132.3, 130.4, 129.4, 128.9, 128.5, 128.2, 127.8, 124.7, 120.9, 120.6, 120.2, 119.1, 111.6, 51.2, 17.5; FT-IR: 3389.50, 3294.16, 1738.88, 1625.66, 1491.81, 1438.23, 1491.81, 1332.54, 1322.30, 1229.78, 1110.42, 851.03, 747.76 cm^{-1}; MS (ESI): m/z 432 [M+H]$^+$, HRMS calculated for $C_{21}H_{17}N_3F_3S_2$ m/z 432.08105 [M+H]$^+$, found m/z 432.08042.

4.8.8. Allyl ((1-(4-(trifluoromethyl)phenyl)-9*H*-pyrido[3,4-*b*]-indol-3-yl)methyl)carbamodithioate (8h)

White solid: 88% yield; mp: 188–192 °C; ^{1}H NMR (300 MHz, $CDCl_3$) δ (ppm): 8.71 (br s, 0.8H), 8.52 (br s, 1H), 8.13 (d, J = 7.9 Hz, 1H), 8.06 (d, J = 7.9 Hz, 2H), 7.91 (s, 1H), 7.85 (d, J = 8.1 Hz, 1.7H), 7.59 (t, J = 7.6 Hz, 1H), 7.52 (d, J = 8.1 Hz, 1H), 7.34 (t, J = 7.5 Hz, 1H), 5.98–5.88 (m, 1H), 5.3 (d, J = 17.1 Hz, 1H), 5.18 (d, J = 4.3 Hz, 1.7H), 5.13 (d, J = 9.9 Hz, 1H), 3.96 (s, 1.7H) and peaks at 8.90, 7.80, 4.92 and 4.10 are due to 15% minor rotamer; ^{13}C NMR (75 MHz, $CDCl_3$ + DMSO-d_6) δ (ppm): 195.8, 143.3, 141.3, 141.2, 139.1, 132.3, 130.4, 129.0, 128.6, 128.2, 127.9, 124.8, 121.6, 121.0, 120.6, 120.2, 119.0, 117.5, 111.6, 51.3, 37.3; FT-IR: 3398.05, 3259.43, 1738.89, 1623.97, 1493.40, 1396.98, 1320.80, 1233.66, 1154.66, 1068.51, 1108.71, 850.92, 739.03 cm^{-1}; MS (ESI): m/z 458 [M+H]$^+$, HRMS calculated for $C_{23}H_{19}N_3F_3S_2$ m/z 458.09670 [M+H]$^+$, found m/z 458.09634.

4.8.9. Benzyl ((1-(4-(trifluoromethyl)phenyl)-9*H*-pyrido[3,4-*b*]indol-3-yl)methyl)carbamodithioate (8i)

Off white solid: 82% yield; mp: 196–200 °C; ^{1}H NMR (500 MHz, $CDCl_3$) δ (ppm): 8.70 (br s, 0.8H), 8.51 (br s, 1H), 8.15 (d, J = 7.8 Hz, 1H), 8.07 (d, J = 7.6 Hz, 2H), 7.97 (s, 1H), 7.86 (d, J = 7.8 Hz, 2H), 7.62–7.51 (m, 2H), 7.40–7.33 (m, 3H), 7.30–7.21 (m, 3H), 5.22 (d, J = 4.3 Hz, 1.7H), 4.59 (s, 1.7H) and peak at 8.90, 4.95 and 4.68 are due to 15% minor rotamer; ^{13}C NMR (75 MHz, $CDCl_3$ + DMSO-d_6) δ (ppm): 196.3, 156.5, 143.2, 141.5, 141.4, 136.2, 135.7, 132.7, 130.9, 130.0, 129.1, 128.6, 128.3, 128.1, 126.9, 125.2, 121.2, 120.6, 119.5, 112.3, 111.9, 51.5, 39.9; FT-IR: 3415.74, 3290.78, 1627.48, 1568.88, 1495.42, 1397.88, 1319.00, 1241.30, 1175.09, 1110.59, 1065.20, 851.13, 748.53 cm^{-1}; MS (ESI): m/z 508 [M+H]$^+$, HRMS calculated for $C_{27}H_{21}N_3F_3S_2$ m/z 508.11235 [M+H]$^+$, found m/z 508.11199.

4.8.10. Methyl ((1-(4-fluorophenyl)-9*H*-pyrido[3,4-*b*]indol-3-yl)methyl)carbamodithioate (8j)

Cream color solid: 68% yield; mp: 200–204 °C; ^{1}H NMR (500 MHz, $CDCl_3$) δ (ppm): 8.73 (br s, 0.9H), 8.42 (br s, 1H), 8.16 (d, J = 7.9 Hz, 1H), 7.96 (q, J = 5.3, 8.4 Hz, 2H), 7.93 (s, 0.8H), 7.59 (t, J = 7.8 Hz, 1H), 7.52 (d, J = 8.1 Hz, 1H), 7.36–7.30 (m, 3H), 5.20 (d, J = 4.3 Hz, 1.7H), 2.69 (s, 2.6H) and peak at 8.91, 8.42, 7.89, 4.96 and 2.76 are due to 15% minor rotamer; ^{13}C NMR (75 MHz, $CDCl_3$ + DMSO-d_6) δ (ppm): 197.4, 163.9 and 160.6 (d, J = 247.5 Hz), 143.3, 141.3, 140.1, 133.9, 132.3, 130.3, 129.9 (d, J = 8.2 Hz), 127.8, 120.9, 120.5, 119.2, 115.1 (d, J = 21.5 Hz), 111.7, 111.5, 51.3, 17.4; FT-IR: 3404.52, 3231.34, 1625.03, 1489.11, 1468.83, 1438.67, 1321.51, 1221.93, 1154.53, 843.31, 740.14 cm^{-1}; MS (ESI): m/z 382 [M+H]$^+$, HRMS calculated for $C_{20}H_{17}N_3FS_2$ m/z 382.08424 [M+H]$^+$, found m/z 382.08464.

4.8.11. Allyl ((1-(4-fluorophenyl)-9*H*-pyrido[3,4-*b*]indol-3-yl)-methyl)carbamodithioate (8k)

Cream color solid: 70% yield; mp: 110–115 °C; ^{1}H NMR (500 MHz, $CDCl_3$) δ (ppm): 8.74 (br s, 0.9H), 8.47 (br s, 1H), 8.13 (d, J = 7.8 Hz, 1H), 7.94 (q, J = 5.5, 7.9 Hz, 2H), 7.89 (s, 0.9H), 7.58 (t, J = 7.5 Hz, 1H), 7.51 (d, J = 7.9 Hz, 1H), 7.34–7.28 (m, 3H), 5.98–5.88 (m, 1H), 5.3 (d, J = 16.9 Hz, 1H), 5.17 (d, J = 3.9 Hz, 1.7H), 5.13 (d, J = 10.1 Hz, 1H), 3.96 (s, 1.7H) and peaks at 8.91, 7.84, 4.93 and 4.10 are due to 15% minor rotamer; ^{13}C NMR (125 MHz, $CDCl_3$) δ (ppm): 196.1, 164.1 and 162.1 (d, J = 248.8 Hz), 143.7, 140.9, 140.6, 134.0, 132.7, 132.6, 131.2, 129.9 (d, J = 8.2 Hz), 128.9, 121.9, 121.5, 120.5, 118.5, 116.2 (d, J = 21.8 Hz), 112.1, 111.6, 51.6, 38.3; FT-IR: 3271.91, 3440.25, 1627.83, 1604.55, 1508.73, 1436.12, 1272.97, 1224.07, 1147.36, 842.76, 738.84 cm^{-1}; MS (ESI): m/z 408 [M+H]$^+$, HRMS calculated for $C_{22}H_{17}N_3FS_2$ m/z 408.09989 [M+H]$^+$, found m/z 408.09962.

4.8.12. Benzyl ((1-(4-fluorophenyl)-9*H*-pyrido[3,4-*b*]indol-3-yl)-methyl)carbamodithioate (8l)

Off white solid: 76% yield; mp: 185–190 °C; ^{1}H NMR (500 MHz, $CDCl_3$) δ (ppm): 8.73 (br s, 0.8H), 8.43 (br s, 1H), 8.14 (d, J = 7.9 Hz, 1H), 7.92 (q, J = 5.5, 8.5 Hz, 2H), 7.91 (s, 0.8H), 7.58 (t, J = 7.8 Hz, 1H), 7.50 (d, J = 8.1 Hz, 1H), 7.39 (d, J = 7.2 Hz, 1.7H), 7.35–7.22 (m, 6H), 5.19 (d, J = 4.3 Hz, 1.7H), 4.58 (s, 1.7H) and peak at 8.92, 7.84, 7.44, 4.93 and 4.68 are due to 15% minor rotamer; ^{13}C NMR (75 MHz, DMSO-d_6 + $CDCl_3$) δ (ppm): 196.1, 163.9 and 160.6 (d, J = 248.1 Hz), 143.1, 141.3, 141.3, 140.1, 136.1, 133.8, 132.2, 130.3, 129.9 (d, J = 8.2 Hz), 128.4, 127.9, 126.7, 120.9, 120.5, 119.2, 115.1 (d, J = 21.5 Hz), 111.8, 111.5, 51.4, 38.9; FT-IR: 3252.72, 1625.44, 1607.01, 1509.33, 1491.46, 1442.14, 1321.00, 1232.77, 843.77, 738.84 cm^{-1}; MS (ESI): m/z 458 [M+H]$^+$, HRMS calculated for $C_{26}H_{21}N_3FS_2$ m/z 458.11554 [M+H]$^+$, found m/z 458.11526.

4.8.13. Methyl ((9-methyl-1-(3,4,5-trimethoxyphenyl)-9*H*-pyrido[3,4-*b*]indol-3-yl)methyl)carbamodithioate (13a)

Light brown solid: 85% yield; mp: 165–170 °C; ^{1}H NMR (300 MHz, $CDCl_3$) δ (ppm): 8.68 (br s, 0.8H), 8.18 (d, J = 7.7 Hz, 1H), 8.00 (s, 0.8H), 7.64 (t, J = 7.5 Hz, 1H), 7.45 (d, J = 8.3 Hz, 1H), 7.34 (t, J = 7.5 Hz, 1H), 6.86 (s, 1.7H), 5.20 (d, J = 4.5 Hz, 1.7H), 3.96 (s, 3H), 3.93 (s, 6H), 3.54 (s, 3H), 2.66 (s, 2.5H) and peaks at 8.81, 7.95, 6.83, 4.95 and 2.75 are due to 15% minor rotamer; ^{13}C NMR (75 MHz, $CDCl_3$) δ (ppm): 197.6, 159.9, 143.5, 142.5, 134.6, 131.7, 131.3, 130.8, 128.8, 121.6, 120.9, 119.9, 113.6, 111.6, 111.2, 109.8, 55.4, 51.5, 32.9, 18.0; FT-IR: 3144.68, 2921.18, 2851.41, 1739.33, 1622.86, 1581.94, 1461.81, 1363.52, 1230.97, 1121.34 cm^{-1}; MS (ESI): m/z 468 $[M+H]^+$, HRMS calculated for $C_{24}H_{26}O_3N_3S_2$ m/z 468.14101 $[M+H]^+$, found m/z 468.14084.

4.8.14. Allyl ((9-methyl-1-(3,4,5-trimethoxyphenyl)-9*H*-pyrido[3,4-*b*]indol-3-yl)methyl)carbamodithioate (13b)

Light brown solid: 86% yield; mp: 136–140 °C; ^{1}H NMR (300 MHz, $CDCl_3$) δ (ppm): 8.66 (br s, 0.9H), 8.18 (d, J = 7.8 Hz, 1H), 7.98 (s, 0.9H), 7.64 (t, J = 8.2 Hz, 1H), 7.44 (d, J = 8.4 Hz, 1H), 7.34 (t, J = 7.5 Hz, 1H), 6.85 (s, 1.8H), 5.96–5.86 (m, 1H), 5.28 (d, J = 16.9 Hz, 1H), 5.19 (d, J = 4.4 Hz, 1.8H), 5.11 (d, J = 10.1 Hz, 1H), 3.96 (s, 2.6H), 3.92 (s, 5.4H), 3.54 (s, 3H) and peaks at 8.80, 7.94, 6.83, 4.95, 3.95 and 3.94 are due to 10% minor rotamer; ^{13}C NMR (125 MHz, $CDCl_3$) δ (ppm): 196.3, 153.1, 143.6, 142.6, 142.3, 138.5, 134.3, 132.6, 131.6, 129.2, 121.8, 120.7, 120.3, 118.4, 112.5, 109.9, 106.9, 106.8, 61.0, 56.3, 51.2, 38.2, 32.8; FT-IR: 3126.39, 2934.07, 1734.98, 1622.99, 1583.11, 1462.53, 1365.58, 1232.41, 1126.96 cm^{-1}; MS (ESI): m/z 494 $[M+H]^+$, HRMS calculated for $C_{26}H_{28}O_3N_3S_2$ m/z 494.15666 $[M+H]^+$, found m/z 494.15662.

4.8.15. Benzyl ((9-methyl-1-(3,4,5-trimethoxyphenyl)-9*H*-pyrido[3,4-*b*]indol-3-yl)methyl)carbamodithioate (13c)

Light brown solid: 88% yield; mp: 165–168 °C; ^{1}H NMR (500 MHz, $CDCl_3$) δ (ppm): 8.69 (br s, 0.8H), 8.18 (d, J = 7.8 Hz, 1H), 7.99 (s, 0.8H), 7.64 (t, J = 7.5 Hz, 1H), 7.44 (d, J = 8.2 Hz, 1H), 7.38–7.32 (m, 3H), 7.29–7.21 (m, 3H), 6.83 (s, 2H), 5.20 (d, J = 3.8 Hz, 1.7H), 4.57 (s, 1.7H), 3.94 (s, 3H), 3.90 (s, 5.1H), 3.53 (s, 3H) and peaks at 8.81, 7.91, 4.94, 4.67 and 3.92 are due to 15% minor rotamer; ^{13}C NMR (125 MHz, $CDCl_3$) δ (ppm): 196.5, 153.1, 143.5, 142.8, 142.5, 138.4, 136.6, 134.5, 134.4, 131.4, 129.3, 129.0, 128.5, 127.4, 121.7, 120.8, 120.2, 112.2, 109.8, 106.9, 61.0, 56.2, 51.6, 39.8, 32.8; FT-IR: 3134.80, 2938.05, 2840.39, 1737.92, 1624.27, 1582.36, 1503.80, 1365.04, 1235.05, 1121.66 cm^{-1}; MS (ESI): m/z 544 $[M+H]^+$, HRMS calculated for $C_{30}H_{30}O_3N_3S_2$ m/z 544.17231 $[M+H]^+$, found m/z 544.17260.

4.8.16. Methyl ((1-(4-methoxyphenyl)-9-methyl-9*H*-pyrido[3,4-*b*]indol-3-yl)methyl)carbamodithioate (13d)

Cream color solid: 85% yield; mp: 168–174 °C; ^{1}H NMR (300 MHz, CD_6CO) δ (ppm): 9.52 (br s, 1H), 8.27 (d, J = 7.9 Hz, 1H), 8.12 (s, 1H), 7.68–7.57 (m, 4H), 7.31 (t, J = 7.7 Hz, 1H), 7.13 (d, J = 8.7 Hz, 2H), 5.16 (d, J = 4.5 Hz, 1.8H), 3.92 (s, 3H), 3.57 (s, 3H), 2.62 (s, 2.6H), and peaks at 4.95 and 2.64 are due to 10% minor rotamer; ^{13}C NMR (75 MHz, $CDCl_3$) δ (ppm): 197.6, 159.9, 143.5, 142.5, 134.6, 131.7, 131.2, 130.8, 128.7, 121.6, 120.8, 119.9, 113.6, 111.6, 111.2, 109.8, 55.3, 51.4, 32.9, 18.0; FT-IR: 3132.08, 2933.45, 2915.13, 2832.11, 1738.77, 1609.20, 1511.74, 350.88, 1245.65, 1177.07 cm^{-1}; MS (ESI): m/z 408 $[M+H]^+$, HRMS calculated for $C_{22}H_{22}ON_3S_2$ m/z 408.11988 $[M+H]^+$, found m/z 408.11927.

4.8.17. Allyl ((1-(4-methoxyphenyl)-9-methyl-9*H*-pyrido[3,4-*b*]-indol-3-yl)methyl)carbamodithioate (13e)

Off white solid: 74% yield; mp: 138–142 °C; ^{1}H NMR (300 MHz, DMSO-d_6) δ (ppm): 10.51 (bt, 0.9H), 8.27 (d, J = 7.6 Hz, 1H), 8.04 (s, 1H), 7.65–7.62 (m, 2H), 7.58 (d, J = 8.5 Hz, 2H), 7.33–7.29 (m, 1H), 7.11 (d, J = 8.5 Hz, 2H), 5.93–5.85 (m, 1H), 5.29 (d, J = 16.9 Hz, 1H), 5.11 (d, J = 9.9 Hz, 1H), 5.06 (d, J = 5.3 Hz, 1.8H), 3.93 (d, J = 6.9 Hz, 2H), 3.86 (s, 3H), 3.48 (s, 3H) and peaks at 10.58 and 4.84 are due to 10% minor rotamer; ^{13}C NMR (75 MHz, DMSO-d_6) δ (ppm): 195.9, 159.3, 144.2, 142.9, 142.7, 133.5, 133.3, 131.0, 129.9, 128.6, 121.5, 120.2, 119.8, 118.1, 113.3, 111.5, 110.5, 55.2, 51.7, 37.0, 32.8; FT-IR: 3157.98, 3005.68, 2925.56, 1738.31, 1606.80, 1488.42, 1509.83, 1439.74, 1376.89, 1310.32, 1250.51, 1127.84 cm^{-1}; MS (ESI): m/z 434 $[M+H]^+$, HRMS calculated for $C_{24}H_{24}ON_3S_2$ m/z 434.13553 $[M+H]^+$, found m/z 434.13498.

4.8.18. Benzyl ((1-(4-methoxyphenyl)-9-methyl-9*H*-pyrido[3,4-*b*]indol-3-yl)methyl)carbamodithioate (13f)

Off white solid: 78% yield; mp: 150–155 °C; ^{1}H NMR (500 MHz, CD_6CO) δ (ppm): 9.56 (br s, 0.9H), 8.25 (d, J = 7.8 Hz, 1H), 8.10 (s, 0.9H), 7.66–7.57 (m, 4H), 7.41 (d, J = 7.3 Hz, 1.8H), 7.33–7.22 (m, 4H), 7.11 (d, J = 8.8 Hz, 2H), 5.18–5.16 (m, 1.8H), 4.59 (s, 1.8H), 4.90 (s, 2.7H), 3.56 (s, 3H) and peaks at 9.60, 8.01, 7.45, 4.95, 4.65 and 3.91 are due to 10% minor rotamer; ^{13}C NMR (75 MHz, $CDCl_3$) δ (ppm): 196.2, 159.9, 143.5, 142.6, 142.1, 136.3, 134.4, 131.3, 130.8, 128.9, 128.4, 127.2, 121.6, 120.7, 120.0, 113.5, 111.9, 111.2, 109.8, 55.2, 51.2, 39.6, 32.8; FT-IR: 3269.38, 3001.87, 2935.17, 2834.77, 1738.85, 1607.97, 1493.70, 1443.56, 1304.72, 1245.81, 1108.53 cm^{-1}; MS (ESI): m/z 484 $[M+H]^+$, HRMS calculated for $C_{28}H_{26}ON_3S_2$ m/z 484.15118 $[M+H]^+$, found m/z 484.15138.

4.8.19. Methyl ((9-methyl-1-(4-(trifluoromethyl)phenyl)-9*H*-pyrido[3,4-*b*]indol-3-yl)methyl)carbamodithioate (13g)

Cream color solid: 80% yield; mp: 202–214 °C; ^{1}H NMR (500 MHz, $CDCl_3$) δ (ppm): 8.62 (br s, 0.8H), 8.19 (d, J = 7.9 Hz, 1H), 8.01 (s, 0.8H), 7.85–7.77 (m, 4H), 7.65 (t, J = 8.2 Hz, 1H), 7.44 (d, J = 8.4 Hz, 1H), 7.35 (t, J = 7.8 Hz, 1H), 5.92 (d, J = 4.4 Hz, 1.7H), 3.48 (s, 3H), 2.65 (s, 2.5H), and peaks at 8.83, 7.97, 4.95 and 2.74 are due to 15% minor rotamer; ^{13}C NMR (125 MHz, $CDCl_3$) (ppm): 197.9, 143.5, 143.0, 142.9, 141.1, 134.6, 131.7, 130.7, 130.0, 129.1, 125.1 (q, J = 2.7 Hz), 122.9, 121.7, 120.7, 120.3, 112.5, 109.8, 51.4, 33.2, 18.0; FT-IR: 3272.66, 2848.89, 1619.83, 1559.84, 1493.18, 1467.31, 1327.20, 1228.88, 1156.26, 1107.19, 1068.07, 841.91, 748.51 cm^{-1}; MS (ESI): m/z 446 $[M+H]^+$, HRMS calculated for $C_{22}H_{19}N_3F_3S_2$ m/z 446.09670 $[M+H]^+$, found m/z 446.09573.

4.8.20. Allyl ((9-methyl-1-(4-(trifluoromethyl)phenyl)-9*H*-pyrido[3,4-*b*]indol-3-yl)methyl)carbamodithioate (13h)

Off white solid: 82% yield; mp: 173–176 °C; ^{1}H NMR (500 MHz, $CDCl_3$) δ (ppm): 8.62 (br s, 0.9H), 8.18 (d, J = 7.8 Hz, 1H), 7.99 (s, 0.9H), 7.84–7.77 (m, 4H), 7.65 (t, J = 7.8 Hz, 1H), 7.44 (d, J = 8.2 Hz, 1H), 7.35 (t, J = 7.5 Hz, 1H), 5.98–5.84 (m, 1H), 5.26 (d, J = 16.9 Hz, 1H), 5.18 (d, J = 4.4 Hz, 1.8H), 5.10 (d, J = 9.9 Hz, 1H), 3.93 (d, J = 6.8 Hz, 1.8H), 3.47 (s, 3H) and peaks at 8.81, 7.95, 4.95 and 4.09 are due to 10% minor rotamer; ^{13}C NMR (125 MHz, $CDCl_3$) (ppm): 196.2, 143.5, 142.9, 141.1, 134.6, 132.6, 131.7, 130.8, 130.5, 130.0, 129.2, 125.1 (q, J = 2.7 Hz), 122.9, 121.7, 120.7, 120.3, 118.4, 112.4, 109.8, 51.4, 38.2, 33.2; FT-IR: 3137.68, 2884.98, 1619.15, 1561.23, 1467.52, 1322.91, 1252.12, 1124.09, 841.96, 749.97 cm^{-1}; MS (ESI): m/z 472 $[M+H]^+$, HRMS calculated for $C_{24}H_{21}N_3F_3S_2$ m/z 472.11235 $[M+H]^+$, found m/z 472.11167.

4.8.21. Benzyl ((9-methyl-1-(4-(trifluoromethyl)phenyl)-9*H*-pyrido[3,4-*b*]indol-3-yl)methyl)carbamodithioate (13i)

Cream color solid: 85% yield; mp: 156–160 °C; ^{1}H NMR (500 MHz, $CDCl_3$) δ (ppm): 8.60 (br s, 0.8H), 8.18 (d, J = 7.8 Hz, 1H), 7.98 (s, 0.8H), 7.82–7.74 (m, 4H), 7.65 (t, J = 8.1 Hz, 1H), 7.44 (d, J = 8.2 Hz, 1H), 7.38–7.33 (m, 3H), 7.30–7.22 (m, 3H), 5.19

(d, J = 3.9 Hz, 1.7H), 4.56 (s, 1.7H) 3.47 (s, 3H) and peaks at 8.82, 7.93, 4.93 and 4.66 are due to 15% minor rotamer; ^{13}C NMR (125 MHz, $CDCl_3$) (ppm): 196.4, 143.5, 142.8, 141.1, 136.4, 134.5, 131.7, 130.7, 130.4, 130.0, 129.2, 129.1, 128.9, 128.5, 127.3, 125.1 (q, J = 2.7 Hz), 121.7, 120.7, 120.3, 112.4, 109.8, 51.5, 39.8, 33.2; FT-IR: 3130.49, 2945.21, 1622.60, 1491.29, 1469.27, 1392.85, 1322.33, 1165.40, 1108.39, 1066.53, 843.53, 746.71 cm^{-1}; MS (ESI): m/z 522 $[M+H]^+$, HRMS calculated for $C_{28}H_{23}N_3F_3S_2$ m/z 522.12800 $[M+H]^+$, found m/z 522.12768.

4.8.22. Methyl ((1-(4-fluorophenyl)-9-methyl-9*H*-pyrido[3,4-*b*]-indol-3-yl)methyl)carbamodithioate (13j)

White solid: 78% yield; mp: 174–178 °C; ^{1}H NMR (500 MHz, $CDCl_3$) δ (ppm): 8.68 (br s, 0.8H), 8.17 (d, J = 7.8 Hz, 1H), 7.96 (d, J = 3.7 Hz, 0.8H), 7.65–7.60 (m, 3H), 7.43 (d, J = 8.2 Hz, 1H), 7.33 (t, J = 7.3 Hz, 1H), 7.26–7.22 (m, 2H), 5.17 (t, J = 3.1 Hz, 1.7H), 3.47 (s, 3H), 2.65 (s, 2.5H) and peaks at 8.84, 7.92, 4.93 and 2.74 are due to 15% minor rotamer; ^{13}C NMR (125 MHz, $CDCl_3$) (ppm): 197.7, 163.9 and 161.9 (d, J = 247.9 Hz), 143.5, 142.7, 141.8, 135.3, 134.5, 131.4, 131.3 (d, J = 8.2 Hz), 128.9, 121.7, 120.8, 120.1, 115.2 (d, J = 20.9 Hz), 112.1, 109.8, 51.4, 32.9, 18.0; FT-IR: 3151.81, 2800.26, 1621.65, 1558.31, 1505.99, 1442.33, 1383.71, 1214.06, 1151.48, 1050.13, 935.05, 833.79, 750.82 cm^{-1}; MS (ESI): m/z 396 $[M+H]^+$, HRMS calculated for $C_{21}H_{19}N_3FS_2$ m/z 396.09989 $[M+H]^+$, found m/z 396.10036.

4.8.23. Allyl ((1-(4-fluorophenyl)-9-methyl-9*H*-pyrido[3,4-*b*]-indol-3-yl)methyl)carbamodithioate (13k)

Off white solid: 85% yield; mp: 133–137 °C; ^{1}H NMR (500 MHz, $CDCl_3$) δ (ppm): 8.68 (br s, 0.8H), 8.17 (d, J = 7.9 Hz, 1H), 7.96 (s, 0.9H), 7.65–7.60 (m, 3H), 7.43 (d, J = 8.4 Hz, 1H), 7.33 (t, J = 7.3 Hz, 1H), 7.25–7.22 (m, 2H), 5.94–5.85 (m, 1H), 5.26 (d, J = 16.9 Hz, 1H), 5.17 (d, J = 4.3 Hz, 1.8H), 5.10 (d, J = 10.1 Hz, 1H), 3.92 (d, J = 6.9 Hz, 1.8H), 3.48 (s, 3H) and peaks at 8.81, 7.92, 4.94 and 4.09 are due to 10% minor rotamer; ^{13}C NMR (125 MHz, $CDCl_3$) (ppm): 196.0, 163.9 and 161.9 (d, J = 247.9 Hz), 143.5, 142.6, 141.8, 135.4, 134.6, 132.6, 131.4, 131.3 (d, J = 8.2 Hz), 128.9, 121.6, 120.8, 120.1, 118.4, 115.2 (d, J = 20.9 Hz), 112.0, 109.8, 51.5, 38.2, 32.9; FT-IR: 3133.80, 2870.76, 1622.41, 1506.64, 1465.05, 1349.74, 1250.40, 1219.29, 1151.05, 1050.44, 929.96, 835.81, 750.38 cm^{-1}; MS (ESI): m/z 422 $[M+H]^+$, HRMS calculated for $C_{23}H_{21}N_3FS_2$ m/z 422.11554 $[M+H]^+$, found m/z 422.11546.

4.8.24. Benzyl ((1-(4-fluorophenyl)-9-methyl-9*H*-pyrido[3,4-*b*]-indol-3-yl)methyl)carbamodithioate (13l)

White solid: 80% yield; mp: 151–155 °C; ^{1}H NMR (500 MHz, $CDCl_3$) δ (ppm): 8.67 (br s, 0.8H), 8.17 (d, J = 7.9 Hz, 1H), 7.94 (s, 0.8H), 7.65–7.58 (m, 3H), 7.42 (d, J = 8.2 Hz, 1H), 7.37–7.31 (m, 3H), 7.29–7.20 (m, 5H), 5.17 (d, J = 3.9 Hz, 1.7H), 4.55 (s, 1.7H), 3.47 (s, 3H) and peaks at 8.83, 7.89, 4.92 and 4.66 are due to 15% minor rotamer; ^{13}C NMR (125 MHz, $CDCl_3$) (ppm): 196.3, 163.9 and 161.9 (d, J = 248.8 Hz), 143.5, 142.6, 141.8, 136.4, 135.3, 134.5, 131.4, 131.3 (d, J = 8.2 Hz), 129.2, 128.9, 128.5, 127.3, 121.7, 120.8, 120.1, 115.2 (d, J = 21.8 Hz), 112.0, 109.8, 51.5, 39.8, 32.9; FT-IR: 3063.55, 2836.71, 1897.72, 1624.23, 1509.15, 1386.26, 1220.92, 1151.95, 1051.90, 927.89, 836.00, 746.68 cm^{-1}; MS (ESI): m/z 472 $[M+H]^+$, HRMS calculated for $C_{27}H_{23}N_3FS_2$ m/z 472.13119 $[M+H]^+$, found m/z 472.13080.

4.9. Biological methods

4.9.1. MTT assay

The anticancer activities of the complexes were determined using MTT assay.[50,51] Cancer cells (DU-145, MCF-7 HeLa and A549) were used in this assay. 1×10^4 cells/well were seeded in 200 μl Dulbecco's modified Eagle's medium (DMEM), supplemented with 10% FBS in each well of 96-well microculture plates and incubated for 24 h at 37 °C in a CO_2 incubator. All the derivatives diluted to the desired concentrations (500 nM, 1 μM, 5 μM, 10 μM, 25 μM, 50 μM, 75 μM, 100 μM, 150 μM) in culture medium, were added to the wells with respective vehicle control. Doxorubicin treated cells, in the same concentration range were used as control. After 48 h of incubation, 10 μl MTT (3-(4,5-dime thylthiazol-2-yl)−2,5-diphenyl tetrazolium bromide) (5 mg/ml) was added to each well and the plates were further incubated for 4 h. Then the supernatant from each well was carefully removed, formazan crystals were dissolved in 100 μl of DMSO and absorbance at 570 nm wavelength was recorded at a wavelength of 540 nm using an ELx800 microplate reader (BioTek, USA).

4.9.2. Cell cycle analysis

Flow cytometry analysis (FACS) was performed to evaluate the distribution of the cells through the cell cycle phases. DU-145 cancer cells were incubated with **8j** and **13g** at 0.5 and 1.0 μM concentrations for 48 h. Untreated DU-145 cells were used as control. Untreated and treated cells were harvested, washed with PBS, fixed in ice-cold 70% ethanol and stained with Propidium Iodide (PI) (Sigma Aldrich). Cell cycle was performed by flow cytometry (Becton Dickinson FACS Caliber) as earlier described.[52]

4.9.3. Annexin V-FITC assay

DU-145 cells (1×10^6) were seeded in six-well plates and allowed to grow overnight. The medium was then replaced with complete medium containing 0.5 and 1 μM concentrations of **8j** and **13g** for 48 h along with vehicle alone (1:1 DMSO/water) as control. After 48 h of drug treatment, cells from the supernatant and adherent monolayer cells were harvested by trypsinization, washed with PBS at 3000 rpm. Then the cells (1×10^6) were stained with Annexin V-FITC and Propidium Iodide using the Annexin-V-PI apoptosis detection kit (Sigma Aldrich, India). Flow cytometry was performed using a FACScan (Becton Dickinson) equipped with a single 488-nm argon laser as described earlier.[53] Annexin V-FITC was analyzed using excitation and emission settings of 488 nm and 535 nm (FL-1 channel); PropidiumIodide, 488 nm and 610 nm (FL-2 channel). Debris and clumps were gated out using forward and orthogonal light scatter.

4.9.4. Morphological analysis by Hoechst staining

Cells were seeded at a density of 10,000 cells over 18-mm cover slips and incubated for 24 h. After incubation, cells were treated with the complexes **8j** and **13g** at 0.5 and 1 μM concentration for 48 h. Hoechst 33258 (Sigma Aldrich) was added to the cells at a concentration of 0.5 mg/ml and incubated for 30 min at 37 °C. Later, DU-145 cells were washed with phosphate buffered saline (PBS). Cells from each cover slip were captured from randomly selected fields under a confocal microscope (Leica TCS SP5, Heidelberg, Germany) to qualitatively determine the proportion of viable and apoptotic cells based on their relative fluorescence and nuclear fragmentation.[54]

4.9.5. DNA-topo II inhibition assay

Topoisomerase II inhibition assay was determined by the ATP dependent decatenation of kDNA. Reactions were carried out in 20 μl and contained 120 mM KCl, 50 mM Tris–HCl, pH 8, 10 mM $MgCl_2$, 0.5 mM dithiothreitol, 0.5 mM ATP, 30 mg/ml bovine serum albumin, 200–300 ng of kDNA, and topoisomerase II. The amount of topoisomerase II (5 units) was adjusted in preliminary experiments to decatenate approximately 100% of the kDNA under our assay conditions. The reactions were incubated at 37 °C for 30 min and terminated by the addition of 2 μl of a stop buffer containing 10% (w/v) SDS and 2 μl 0.5 mg/ml proteinase-K and then

incubated for 10 min at 37 °C. After completion of the reaction catenated and decatenated reaction products were separated by 1% agarose gel electrophoresis with ethidium bromide (0.2 μg/ml) as DNA staining agent. Authentic decatenated kDNA and linear kDNA (Topogen Inc.) were run as controls to identify decatenated kDNA. The gels were run at 100 V for about 40 min and visualized under UV transillumination (BIO RAD gel doc XR$^+$, USA).

4.9.6. UV–visible spectroscopy titrations

UV–visible spectroscopy titrations were performed using ABI Lambda 40 UV–Vis spectrophotometer (Foster City, USA) at 25 °C using 1 cm path length quartz cuvette. Stock solutions of 10 μM of CT DNA (calf thymus DNA, which can form perfect double stranded DNA structure) were prepared in 100 mM KBPES buffer (30 mM Potassium Phosphate, pH 7.0, with 100 mM KCl, pH 7.0). 10 μM synthesized derivatives stock solution was prepared by dissolving them in 1:1 DMSO/Milli Q water. UV–visible absorption titrations were done by adding 100 nM CT DNA solution in 100 mM KBPES buffer (pH 7.0) each time to the quartz cuvette containing about 1 μM derivative solution. Titrations were carried out until the complex absorption band remains at a fixed wavelength upon five successive additions of CT DNA. Absorption spectra were recorded from 200 nm to 380 nm.

4.9.7. Fluorescence spectroscopy titrations

Fluorescence emission spectra were measured at 25 °C using a Hitachi F4500 spectrofluorimeter (Maryland, USA) using a 1 cm path length quartz cuvette. Throughout the fluorescence experiment, the concentration of the derivatives was kept constant (10 μM) and titrated with increasing concentrations of CT DNA (from the working solution with 10 μM CT DNA concentration). Fluorescence spectra were recorded after each addition of CT DNA to the fluorescent cuvette. After each experiment, the quartz cuvettes was thoroughly washed with distilled water and dilute nitric acid (approximately 0.1 N, nitric acid) to remove traces of derivative binding to the walls of quartz cuvette. **8j** and **13g** derivatives were excited at 522 nm, and emission spectra for each titration were collected from 550 nm to 650 nm. Each spectrum was recorded three times and the average of three scans was taken.

4.9.8. Circular dichroism (CD) spectroscopy studies

Circular dichroism experiments were carried out using JASCO 815 CD spectropolarimeter (Jasco, Tokyo, Japan). CD spectrum was recorded from 230 to 320 nm to find the conformation of DNA after CT DNA–derivative interaction. For CD experiments, 10×10^{-6} M of CT DNA was used. For characterizing derivative–CT DNA interaction, CD spectra is recorded in 1:0, 1:1 and 1:2 molar ratio of CT DNA/derivative, respectively. CD titrations were performed in 100 mM KBPES buffer (pH 7.0) at 25 °C. Each CD spectrum was recorded thrice and the average of three scans was considered.

Acknowledgements

The authors, M.S., V.S., B.K., Y.T., D.T. and C.B. acknowledge the Council of Scientific and Industrial Research (CSIR), New Delhi (India) for the financial support under the 12th Five Year Plan Project 'Affordable Cancer Therapeutics (ACT)' (CSC0301). N.N. is thankful to the Indo–Swiss Joint Research Programme (ISJRP) for partial financial support (Grant number: CH138844). M.S., V.S. and Y.T. are thankful to the CSIR for providing the research fellowships.

Supplementary data

Supplementary data associated with this article can be found, in the online version, at http://dx.doi.org/10.1016/j.bmc.2015.07.037.

References and notes

1. Beria, I.; Baraldi, P. G.; Cozzi, P.; Caldarelli, M.; Geroni, C.; Marchini, S.; Mongelli, N.; Romagnoli, R. *J. Med. Chem.* **2004**, *47*, 2611.
2. (a) Hurley, L. H. *Nat. Rev. Cancer* **2002**, *2*, 188; (b) Demeunynck, M.; Bailly, C.; Wilson, W. D. In *DNA and RNA Binders: From Small Molecules to Drugs*; Wiley-VCH: Weinheim, 2003; Vols. 1 and 2,; (c) Gurova, K *Future Oncol.* **2009**, *5*, 1685.
3. Kren, V.; Rezanka, T. *FEMS Microbiol. Rev.* **2008**, *32*, 858.
4. Bourdouxhe-Housiaux, C.; Colson, P.; Houssier, C.; Waring, M. J.; Bailly, C. *Biochemistry* **1996**, *35*, 4251.
5. Tu, L. C.; Chen, C. S.; Hsiao, I. C.; Chern, J. W.; Lin, C. H.; Shen, Y. C.; Yeh, S. F. *Chem. Biol.* **2005**, *12*, 1317.
6. Cao, R.; Peng, W.; Wang, Z.; Xu, A. *Curr. Med. Chem.* **2007**, *14*, 479.
7. Xiao, S.; Lin, W.; Wang, C.; Yang, M. *Bioorg. Med. Chem. Lett.* **2001**, *11*, 437.
8. Hayashi, K.; Nagao, M.; Sugimura, T. *Nucleic Acids Res.* **1977**, *4*, 3679.
9. (a) Deveau, A. M.; Labroli, M. A.; Dieckhaus, C. M.; Barthen, M. T.; Smith, K. S.; Macdonald, T. L. *Bioorg. Med. Chem. Lett.* **2001**, *11*, 1251; (b) Zhao, M.; Bi, L.; Wang, W.; Wang, C. *Bioorg. Med. Chem.* **2006**, *14*, 6998; (c) Chaniyara, R.; Tala, S.; Chen, C. W.; Zang, X.; Kakadiya, R.; Lin, L. F.; Chen, C. H.; Chien, S. I.; Chou, T. C.; Tsai, T. H.; Lee, T. C.; Shah, A.; Su, T. L. *J. Med. Chem.* **2013**, *56*, 1544.
10. (a) Song, Y.; Wang, J.; Teng, S. F.; Kesuma, D.; Deng, Y.; Duan, J.; Wang, J. H.; Qi, R. Z.; Sim, M. M. *Bioorg. Med. Chem. Lett.* **2002**, *12*, 1129; (b) Song, Y.; Kesuma, D.; Wang, J.; Deng, Y.; Duan, J.; Wang, J. H.; Qi, R. Z. *Biochem. Biophys. Res. Commun.* **2004**, *317*, 128; (c) Li, Y.; Liang, F.; Jiang, W.; Yu, F.; Cao, R.; Ma, Q.; Dai, X.; Jiang, J.; Wang, Y.; Si, S. *Cancer Biol. Ther.* **2007**, *6*, 1193.
11. Trujillo, J. I.; Meyers, M. J.; Anderson, D. R.; Hegde, S.; Mahoney, M. W.; Vernier, W. F.; Buchler, I. P.; Wu, K. K.; Yang, S.; Hartmann, S. J.; Reitz, D. B. *Bioorg. Med. Chem. Lett.* **2007**, *17*, 4657.
12. (a) Zhang, J.; Li, Y.; Guo, L.; Cao, R.; Zhao, P.; Jiang, W.; Ma, Q.; Yi, H.; Li, Z.; Jiang, J.; Wu, J.; Wang, Y.; Si, S. *Cancer Biol. Ther.* **2009**, *8*, 2374; (b) Han, X.; Zhang, J.; Guo, L.; Cao, R.; Li, Y.; Li, N.; Ma, Q.; Wu, J.; Wang, Y.; Si, S. *PLoS One* **2012**, *7*, e46546. http://www.plosone.org.
13. Barsanti, P. A.; Wang, W.; Ni, Z.; Duhl, D.; Brammeier, N.; Martin, E. *Bioorg. Med. Chem. Lett.* **2010**, *20*, 157.
14. Castro, A. C.; Dang, L. C.; Soucy, F.; Grenier, L.; Mazdiyasni, H.; Hottelet, M.; Parent, L.; Pien, C.; Palombella, V.; Adams, J. *Bioorg. Med. Chem. Lett.* **2003**, *13*, 2419.
15. Martinez, R.; Chacon-Garcia, L. *Curr. Med. Chem.* **2005**, *12*, 127.
16. Wu, J.; Cui, G.; Zhao, M.; Cui, C.; Peng, S. *Mol. Biosyst.* **2007**, *3*, 855.
17. Formagio, Nazari. *Bioorg. Med. Chem.* **2008**, *16*, 9660.
18. Savariz, F. C.; Foglio, M. A.; de Carvalho, J. E.; Ruiz, A. L.; Duarte, M. C.; da Rosa, M. F.; Meyer, E.; Sarragiotto, M. H. *Molecules* **2012**, *17*, 6100.
19. Barbosa, V. A.; Formagio, A. S.; Savariz, F. C.; Foglio, M. A.; Spindola, H. M.; de Carvalho, J. E.; Meyer, E.; Sarragiotto, M. H. *Bioorg. Med. Chem.* **2011**, *19*, 6400.
20. (a) Chen, Z.; Cao, R.; Shi, B.; Yi, W.; Yu, L.; Song, H.; Ren, Z.; Peng, W. *Bioorg. Med. Chem. Lett.* **2010**, *20*, 3876; (b) Chen, Z.; Cao, R.; Shi, B.; Guo, L.; Sun, J.; Mac, Q.; Fan, W.; Song, H. *Eur. J. Med. Chem.* **2011**, *46*, 5127; (c) Chen, Z.; Cao, R.; Yu, L.; Shi, B.; Sun, J.; Guo, L.; Ma, Q.; Yi, W.; Song, X.; Song, H. *Eur. J. Med. Chem.* **2010**, *45*, 4740.
21. Ikeda, R.; Iwaki, T.; Iida, T.; Okabayashi, T.; Nishi, E.; Kurosawa, M.; Sakai, N.; Konakahara, T. *Eur. J. Med. Chem.* **2011**, *46*, 636.
22. Cuny, G. D.; Ulyanova, N. P.; Patnaik, D.; Liu, J. F.; Lin, X.; Auerbach, K.; Ray, S. S.; Xian, J.; Glicksman, M. A.; Stein, R. L.; Higgins, T. M. *Bioorg. Med. Chem. Lett.* **2012**, *22*, 2015.
23. (a) Kamal, A.; Rao, M. P.; Swapna, P.; Srinivasulu, V.; Bagul, C.; Shaik, A. B.; Mullagiri, K.; Kovvuri, J.; Reddy, V. S.; Vidyasagar, K.; Nagesh, N. *Org. Biomol. Chem.* **2014**, *12*, 2370; (b) Shankaraiah, N.; Nekkanti, S.; Chudasama, K. J.; Senwar, K. R.; Sharma, P.; Jeengar, M. K.; Naidu, V. G. M.; Srinivasulu, V.; Kamal, A. *Bioorg. Med. Chem. Lett.* **2014**, *24*, 5413.
24. (a) Kamal, A.; Srinivasulu, V.; Nayak, V. L.; Sathish, M.; Shankaraiah, N.; Bagul, C.; Reddy, N. V.; Rangaraj, N.; Nagesh, N. *Tetrahedron Lett.* **2009**, *50*, 520.
25. Hou, X.; Ge, Z.; Wang, T.; Guo, W.; Cui, J.; Cheng, T.; Lai, C.; Lia, R. *Bioorg. Med. Chem. Lett.* **2006**, *16*, 4214.
26. Zheng, Y. C.; Duan, Y. C.; Ma, J. L.; Xu, R. M.; Zi, X.; Lv, W. L.; Wang, M. M.; Ye, X. W.; Zhu, S.; Mobley, D.; Zhu, Y. Y.; Wang, J. W.; Li, J. F.; Wang, Z. R.; Zhao, W.; Liu, H. M. *J. Med. Chem.* **2013**, *56*, 8543.
27. Gaspari, P.; Banerjee, T.; Malachowski, W. P.; Muller, A. J.; Prendergast, G. C.; DuHadaway, J.; Bennett, S.; Donovan, A. M. *J. Med. Chem.* **2006**, *49*, 684.
28. Gerhäuser, C.; You, M.; Liu, J.; Moriarty, R. M.; Hawthorne, M.; Mehta, R. G.; Moon, R. C.; Pezzuto, J. M. *Cancer Res.* **1997**, *57*, 272.
29. (a) Kamal, A.; Srikanth, Y. V. V.; Shaik, T. B.; Khan, M. N. A.; Ashraf, M.; Reddy, M. K.; Kumar, K. A.; Kalivendi, S. V. *Med. Chem. Commun.* **2011**, *2*, 819; (b) Kamal, A.; Sultana, F.; Ramaiah, M. J.; Srikanth, Y. V. V.; Viswanath, A.; Kishor, C.; Sharma, P.; Pushpavalli, S. N. C. V. L.; Addlagatta, A.; Pal-Bhadra, M. *ChemMedChem* **2012**, *7*, 292; (c) Kamal, A. *Eur. J. Med. Chem.* **2012**, *50*, 9; (d) Kamal, A.; Dastagiri, D.; Ramaiah, M. J.; Reddy, J. S.; Bharathi, E. V.; Srinivas, C.; Pal, D.; Pal-Bhadra, M. *ChemMedChem* **2010**, *5*, 1937.
30. Wilson, J. K.; Sargent, J. M.; Elgie, A. W.; Hill, J. G.; Taylor, C. G. *Br. J. Cancer* **1990**, *62*, 189.
31. Hotz, M. A.; Gong, J.; Traganos, F.; Darzynkiewicz, Z. *Cytometry* **1994**, *15*, 237.
32. Weir, N. M.; Selvendiran, K.; Kutala, V. K.; Tong, L.; Vishwanath, S.; Rajaram, M.; Tridandapani, S.; Anant, S.; Kuppusamy, P. *Cancer Biol. Ther.* **2007**, *6*, 178.
33. Wlodkowic, D.; Skommer, J.; Darzynkiewicz, Z. *Cytometry Part A* **2010**, *77*, 591.
34. Wyllie, A. H. *Nature* **1980**, *284*, 555.
35. Pasternack, R. F.; Cibbs, E. J.; Villafranca, J. J. *Biochemistry* **1983**, *22*, 2406.

36. Barton, J. K.; Dennenberg, J. J.; Chaires, J. B. *Biochemistry* **1993**, *32*, 2573.
37. Wu, J.; Zhao, M.; Qian, K.; Lee, K. H.; Morris-Natschke, S.; Peng, S. *Eur. J. Med. Chem.* **2009**, *44*, 4153.
38. Nyarko, E.; Hanada, N.; Habib, A.; Tabata, M. *Inorg. Chim. Acta* **2004**, *357*, 739.
39. Mahadevan, S.; Palaniandavar, M. *Inorg. Chem.* **1998**, *37*, 693.
40. Raju, G.; Srinivas, R.; Reddy, V. S.; Idris, M. M.; Kamal, A.; Nagesh, N. *PLoS One* **2012**, *7*, e35920.
41. Wang, L.; Wen, Y.; Liu, J.; Zhou, J.; Li, C.; Wei, C. *Org. Biomol. Chem.* **2011**, *9*, 2648.
42. Lipinski, C. A.; Lombardo, F.; Dominy, B. W.; Feeney, P. J. *Adv. Drug Deliv. Rev.* **1997**, *23*, 1.
43. Ertl, P. Calculation of Molecular Properties and Bioactivity Score, Available online: http://www.molinspiration.com (accessed on 31 January 2012).
44. Frisch, M. J.; Trucks, G. W.; Schlegel, H. B.; Scuseria, G. E.; Robb, M. A.; Cheeseman, J. R.; Scalmani, G.; Barone, V.; Mennucci, B.; Petersson, G. A.; Nakatsuji, H.; Caricato, M.; Li, X.; Hratchian, H. P.; Izmaylov, A. F.; Bloino, J.; Zheng, G.; Sonnenberg, J. L.; Hada, M.; Ehara, M.; Toyota, K.; Fukuda, R.; Hasegawa, J.; Ishida, M.; Nakajima, T.; Honda, Y.; Kitao, O.; Nakai, H.; Vreven, T., ; Montgomery, J. A., Jr.; Peralta, J. E.; Ogliaro, F.; Bearpark, M.; Heyd, J. J.; Brothers, E.; Kudin, K. N.; Staroverov, V. N.; Kobayashi, R.; Normand, J.; Raghavachari, K.; Rendell, A.; Burant, J. C.; Iyengar, S. S.; Tomasi, J.; Cossi, M.; Rega, N.; Millam, J. M.; Klene, M.; Knox, J. E.; Cross, J. B.; Bakken, V.; Adamo, C.; Jaramillo, J.; Gomperts, R.; Stratmann, R. E.; Yazyev, O.; Austin, A. J.; Cammi, R.; Pomelli, C.; Ochterski, J. W.; Martin, R. L.; Morokuma, K.; Zakrzewski, V. G.; Voth, G. A.; Salvador, P.; Dannenberg, J. J.; Dapprich, S.; Daniels, A. D.; Farkas, Ö.; Foresman, J. B.; Ortiz, J. V.; Cioslowski, J.; Fox, D. J. *Gaussian 09, Revision B.01*; Gaussian: Wallingford CT, 2009.
45. Morris, G. M.; Huey, R.; Lindstrom, W.; Sanner, M. F.; Belew, R. K.; Goodsell, D. S.; Olson, A. J. *J. Comput. Chem.* **2009**, *30*, 2785.
46. Delano, W. L. *The PyMOL Molecular Graphics System*; DeLano Scientific: San Carlos, CA, 2002.
47. Wei, H.; Ruthenburg, A. J.; Bechis, K. S.; Verdine, G. L. *J. Biol. Chem.* **2005**, *280*, 37041.
48. Temperini, C.; Messori, L.; Orioli, P.; Di Bugno, C.; Animati, F.; Ughetto, G. *Nucleic Acids Res.* **2003**, *31*, 1464.
49. Balendiran, K.; Rao, S.; Sekharudu, C.; Zon, G.; Sundaralingam, M. *Biol. Crystallogr.* **1995**, *51*, 190.
50. Berenyi, A.; Minorics, R.; Ivanyi, Z.; Ocsovszki, I.; Duczaa, E.; Thole, H.; Messinger, J.; Wolfling, J.; Motyan, G.; Mernyak, E.; Frank, E.; Schneider, G.; Zupko, I. *Steroids* **2013**, *78*, 69.
51. Das, B.; Reddy, C. R.; Kashanna, J.; Mamidyala, S. M.; Kumar, C. G. *Med. Chem. Res.* **2012**, *21*, 3321.
52. Szumilak, M.; Szulawska-Mroczek, A.; Koprowska, K.; Stasiak, M.; Lewgowd, W.; Stanczak, A.; Czyz, M. *Eur. J. Med. Chem.* **2010**, *45*, 5744.
53. Browne, L. J.; Gude, C.; Rodriguez, H.; Steele, R. E.; Bhatnager, A. *J. Med. Chem.* **1991**, *34*, 717.
54. Shankar, R.; Chakravarti, B.; Singh, U. S.; Ansari, M. I.; Deshpande, S.; Dwivedi, S. K. D.; Bid, H. K.; Konwar, R.; Kharkwal, G.; Chandra, V.; Dwivedi, A.; Hajela, K. *Bioorg. Med. Chem.* **2009**, *17*, 3847.